The Journal of The Royal Astronomical Society of Canada

Journal

Le Journal de la Société royale d'astronomie du Canada

PROMOTING ASTRONOMY IN CANADA

April/avril 2011
Volume/volume 105
Number/numéro 2 [747]

Inside this issue:

Star trails over Vancouver Island


FREE SHIPPING
To Anywhere in Canada, All Products, Always
canadian telescopes .com
THE BEST
152mm ACHROMAT
NEW FROM
CANADIAN TELESCOPES
Only $739.00
F:5.9 - Fully Multicoated Lens - 3” Deluxe 10:1 Double Speed Focuser
2” Diagonal - Retractable Dew Shield - Collimatable Lens
Universal Mounting Bar - Carry Handle -Metal Lens Cap
CanadianTelescopes.Com
Largest Collection of Telescopes and Accessories from Major Brands

Journal

April/avril 2011 | Vol. 105, No. 2 | Whole Number 747

Royal Astronomical Society of Canada

Société Royale d'Astronomie du Canada

contents / table des matières

Feature Articles / Articles de fond

Departments / Départements

Columns / Rubriques

On the Cover: *Victoria Centre member W. John McDonald set up on the Vancouver Island waterfront and assembled this image of northern star trails in February last year. The assembly is a collection of 30-second images over an 8-hour period through the night. Visible in the lower right are the lights from the homes and ski hills of Vancouver. Boat and plane light trails are also visible in the lower part of the image. John used a Canon T1i camera set at 1600 ISO with a Sigma 10-20-mm f/4 lens operating at 10 mm.*

Journal

The *Journal* is a bi-monthly publication of The Royal Astronomical Society of Canada and is devoted to the advancement of astronomy and allied sciences. It contains articles on Canadian astronomers and current activities of the RASC and its Centres, research and review papers by professional and amateur astronomers, and articles of a historical, biographical, or educational nature of general interest to the astronomical community. All contributions are welcome, but the editors reserve the right to edit material prior to publication. Research papers are reviewed prior to publication, and professional astronomers with institutional affiliations are asked to pay publication charges of $100 per page. Such charges are waived for RASC members who do not have access to professional funds as well as for solicited articles. Manuscripts and other submitted material may be in English or French, and should be sent to the Editor-in-Chief.

The *Journal* of The Royal Astronomical Society of Canada is published at an annual subscription rate of $93.45 (including tax) by The Royal Astronomical Society of Canada. Membership, which includes the publications (for personal use), is open to anyone interested in astronomy. Applications for subscriptions to the *Journal* or membership in the RASC, and information on how to acquire back issues of the *Journal* can be obtained from:

The Royal Astronomical Society of Canada
203 – 4920 Dundas St W
Toronto ON M9A 1B7, Canada
Internet: nationaloffice@rasc.ca
Web site: www.rasc.ca
Telephone: (416) 924-7973
Fax: (416) 924-2911

Canadian Publications Mail Registration No. 09818
Canada Post: Send address changes to 203 - 4920 Dundas St W, Toronto ON M9A 1B7

Canada Post Publication Agreement No. 40069313
We acknowledge the financial support of the Government of Canada through the Canada Periodical Fund (CPF) for our publishing activities.

Canada

The *Journal* is printed on recycled stock.

President's Corner

Mary Lou Whitehorne
President, RASC

As I sit down to write this column for the April issue of the *Journal*, spring seems very far away. It's -14 °C outside and 38 cm of snow just fell with a thud. It's Canada in early February! But by the time you read this, we will be approaching the Spring Equinox. The long dark nights of winter will be giving way to the growing light of spring, and the realm of galaxies will swing across our nighttime view of the heavens. When Leo rides high in the south before midnight, I heave a big sigh of relief that we have not somehow become stuck on the winter side of Earth's orbit around the Sun!

The RASC is also closing in on an important anniversary – the first anniversary of our new Executive Director, Deborah Thompson. An Executive Director is a new experience for the RASC, and we are all a little unsure of how things will be different or the same with our new member on the executive team. Yes, even your executive members are still working out how best to make the new order run as smoothly and efficiently as possible.

But, I can say with complete confidence that the management of our business affairs is in very good hands, with new policy, process, and procedure in place. A great deal of work has been done to establish and maintain best-business practices in our National Office. This all-important groundwork is establishing the sturdy foundation we need to steer the RASC toward a strong and vibrant future as both a charity and a membership organization.

As yet, the changes already in place are not obvious to the average member. They are obvious to the Executive Committee that is involved in day-to-day management and decision making for the Society. One of the biggest changes is that the executive is already benefitting from a reduced workload. Deborah is energetic, scrupulous, and dedicated to the interests of the RASC. She is a pleasure to work with and is a tremendous asset to the RASC. Over time, we will all begin to see the differences and benefits of having a professional manager on the job. I have no doubt that she will continue to implement improvements and be a key player in taking the Society from strength to even greater strength in the future.

Switching topics from business to observing, there have been positive developments on the green-laser-pointer front. These are powerful tools for astronomy education and outreach, but they also pose hazards, particularly to aircraft. In recent months, there has been an increase in the incidence of aircraft *flashing* incidents, with arrests and convictions. Some jurisdictions are moving to outlaw the use of these devices or to ban the importation of green-laser pointers. There is potential for amateur astronomers to be seen as the *bad guys* who use green lasers irresponsibly.

Our Green-Laser Pointer (GLP) Committee has worked hard to research and develop recommended guidelines for the safe, responsible use of green lasers. In consultation with the Executive Committee, the GLP Committee has also authored the RASC's position statement on laser pointers. This is freely available on our Web site at www.rasc.ca/news/article_500.shtml

By the time you read this, members of the GLP and Executive Committees will probably have had a first meeting with Transport Canada officials from Ottawa on this topic. Early indications are that Transport Canada understands our interest in being able to use green-laser pointers. Transport Canada has expressed a desire to work cooperatively with us to reach a reasonable solution to the problem. Thanks to the careful and dedicated work of our volunteers, the RASC may be well positioned to positively influence policy development around the use of such lasers in Canada. This is very good news and could lead to the best possible outcome for astronomy education and outreach throughout the country.

My thanks and appreciation goes to Randall Rosenfeld and members of the GLP Committee, the Executive Committee, Dave Lane, our staff, and all of our members who have contributed and will continue contributing to this important work. I believe the results will be worth the effort.

Lead on, Urania! ✶

News Notes / En Manchettes

compiled by Andrew I. Oakes
(copernicus1543@gmail.com)

Spacecraft returns asteroid samples

A multi-year space mission plagued with malfunctions has succeeded in returning tiny samples of a distant asteroid, three years later than was originally planned.

The perseverance and problem solving of scientists at the Japanese Aerospace Exploration Agency (JAXA) ensured that the *Hayabusa* spacecraft made it home with microscopic pieces of asteroid Itokawa after a prolonged seven-year mission. *Hayabusa (Muses-C)*, which launched on 2003 May 9, achieved its goal of reaching Itokawa and performing scientific observations in 2005. It returned to Earth on 2010 June 13, parachuting its onboard capsule within a prescribed landing zone in Australia, officially ending the mission's technical operations.

Hayabusa, developed specifically to investigate asteroids, was originally scheduled to return in 2007, but a three-year delay ensued due to various malfunctions – a fuel leak, a loss of communications, and the failure of projectiles to fire and blast up dust from the asteroid's surface, almost denying the spacecraft's acquisition of prized samples. The three-year delay also meant the spacecraft stayed longer than expected in the extreme vacuum and cold environment of space, which worried planners about the aging of parachute-release explosives and the possibility of malfunction upon re-entry into the Earth's atmosphere.

The billion-kilometre voyage from Earth to Itokawa took *Hayabusa* a little over two years. In 2005, the spacecraft performed a spectacular feat by landing on the asteroid's surface. Despite the failure of projectiles to fire once the spacecraft was securely on the surface, asteroid particles did make it into the spacecraft's collection chamber, kicked up from the landing itself. The particles were extremely tiny, each smaller than the diameter of a human hair.

A team of scientists removed 2000 particles from the spacecraft's collection chamber, later identifying at least 1500 of them as being part of the asteroid after analysis with an electron microscope.

Asteroid Itokawa is said to be a very primitive-type asteroid. More scientific information on the asteroid was to be provided at the March 2011 Lunar and Planetary Science Conference in Houston.

The *Hayabusa* spacecraft employed a new propulsion technology – an ion engine that first ionizes the propellant gas, xenon, and then electrically accelerates and emits the ions to propel the spacecraft. A highly efficient engine, it is expected to be an important technological tool for future explorations.

Another innovation demonstrated by *Hayabusa* was the Autonomous Navigation System, which enabled the spacecraft to approach the far-away asteroid without human guidance. The navigation system measured the distance to the asteroid with

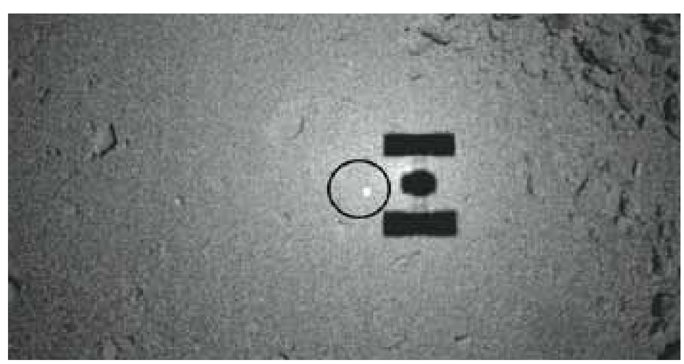

Figure 1 — Hayabusa photographs its own shadow on Asteroid Itokawa in 2005. Photo: Japanese Aerospace Exploration Agency (JAXA)

the Optical Navigation Camera, and used a Light Detection and Ranging (LIDAR) system to refine the approach and later to map the asteroid's surface. LIDAR uses the time-of-flight of a laser pulse to acquire a precise measurement of its distance from the reflecting body.

Asteroid Itokawa is named after the late Dr. Hideo Itokawa, the father of Japan's space-development program.

SOHO provides access to library of solar images

The European Space Agency (ESA) has developed new software that makes available online the entire library of images from the *SOHO SOlar and Heliospheric Observatory*.

JHelioviewer, the new visualisation software developed as part of the ESA/NASA Helioviewer Project, enables users to explore our closest star by providing desktop access to images of the Sun from the past 15 years. More than a million images from *SOHO* can already be accessed, and new images from NASA's *Solar Dynamics Observatory* are being added every day. The downloadable *JHelioviewer* is complemented by a Web-based image browser at Helioviewer.org. The software allows users to create their own movies of the Sun, colour the images as they wish, and image-process the movies in real time. They can also export their finished movies in various formats, and track features on the Sun by compensating for solar rotation.

The *JHelioviewer* software is written in the *Java* programming language, hence the 'J' at the beginning of its name. As open-source software, all its components are freely available, so others can help to improve the program. The code can even be reused for other purposes, such as being applied to Mars data.

"The goal of *JHelioviewer*, and the Helioviewer Project as a whole, is to offer intuitive interfaces to large datasets from many different sources," said Daniel Müller, ESA SOHO Deputy Project Scientist. "In effect, it is a virtual observatory."

Figure 2 — The JHelioviewer Web portal. Image: ESA/NASA Helioviewer Project.

Frost damage brought end to *Phoenix* Mars mission

All good things come to an end. NASA's *Phoenix* mission officially concluded operations in 2010 after repeated attempts to contact the lander were unsuccessful.

Fuk Li, manager of the Mars Exploration Program at NASA's Jet Propulsion Laboratory in Pasadena, California, noted "The *Phoenix* spacecraft succeeded in its investigations and exceeded its planned lifetime. Although its work is finished, analysis of information from *Phoenix*'s science activities will continue for some time to come."

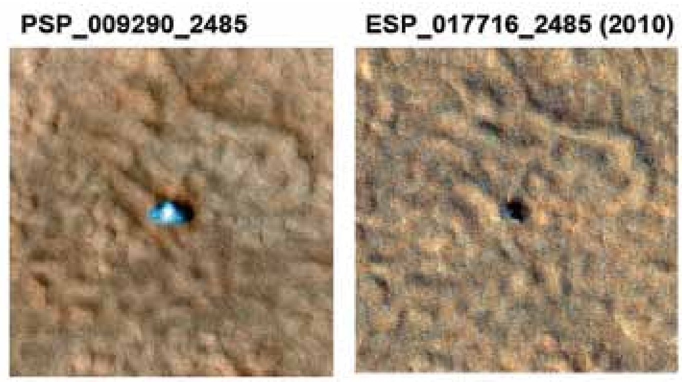

Figure 3 — Two images of the Phoenix *Mars lander taken from Martian orbit in 2008 and 2010. The 2008 lander image (left) shows two relatively blue spots on either side corresponding to the spacecraft's clean circular solar panels. In the 2010 (right) image, scientists see a dark shadow that could be the lander body and eastern solar panel, but no shadow from the western solar panel. Image: NASA/JPL-Caltech/University of Arizona*

In mid-2010, NASA's *Mars Odyssey* orbiter flew over the *Phoenix* landing site 61 times during a final attempt to communicate with the lander. No transmission was detected. *Phoenix* also did not communicate during 150 flights in 3 earlier listening campaigns that year. The spacecraft was not designed to survive the dark, cold, icy winter; however, the slim possibility that *Phoenix* did in fact survive could not be eliminated without listening for the lander after summer sunshine returned.

Phoenix landed during summer conditions at the far-northern site on Mars on 2008 May 25. The solar-powered lander completed its three-month mission and kept working until sunlight waned two months later.

An image of *Phoenix*, taken in May 2010 by the High Resolution Imaging Science Experiment, (HiRISE) camera on board the *Mars Reconnaissance Orbiter* suggested the lander no longer casts shadows the way it did during its working lifetime. The before and after images are dramatically different. According to Michael Mellon of the University of Colorado in Boulder, a science team member for both *Phoenix* and HiRISE, "The lander looks smaller, and only a portion of the difference can be explained by accumulation of dust on the lander, which makes its surfaces less distinguishable from surrounding ground." Project managers anticipated that the weight of a carbon-dioxide ice buildup could bend or break the lander's solar panels. Mellon calculated hundreds of pounds of ice probably coated the lander in mid-winter.

The lander returned a wealth of data for astrobiologists studying the potential for past or present life on Mars. During its mission, the spacecraft confirmed and examined patches of the widespread deposits of underground water ice detected by *Odyssey* and identified a mineral called calcium carbonate that suggested occasional presence of liquid water. It also found soil chemistry with significant implications for life and observed falling snow. The mission's biggest surprise was the discovery of perchlorate, an oxidizing chemical on Earth that is food for some microbes and potentially toxic for others.

New space strategy for Germany

The German Federal Government has adopted a new space strategy to ensure the country's scientific strength and technological leadership in its growing space expertise.

The space strategy defines the fundamentals of how the high-technology space sector is to develop over the next few years at a national level and how it must respond to changing political and societal conditions on the domestic as well as international stages. Adopted towards the end of 2010, the space strategy was drafted jointly with federal German ministries involved in space activities, in consultation with scientific and business establishments such as the German Aerospace Center (DLR).

"Germany's challenge lies in the competition for the best ideas and the best technologies," said Johann-Dietrich Wörner, Chairman of the German Aerospace Center Executive Board. "The advancement of science and technology has to be a core element of our society. It is this need that drives Germany's new space strategy."

"This strategy maps out a path for the future development of the space sector in Germany; one in which [the German Aerospace Center] …, in its capacity as Germany's national space agency and major research centre, has been able to play a significant defining and determining role," said Wörner.

According to a German Aerospace Center statement, over the last few years, space has developed from a science-oriented symbol of technological competition into a means of solving societal problems and global challenges such as climate change and the provision of security. With this premise as a starting point, German space policy and its implementation is focusing on clearly defined objectives. This includes the strategic expansion of national space expertise, to maintain a strong position for German technology in the competitive international marketplace.

The space policy also aims at ensuring that, at the European level, appropriate directives exist to afford the same competitive opportunities to all the countries involved in space activities, thereby creating a strong platform for a future *division of labour* in the European space sector.

This is also relevant for positioning Germany to be able to perform research in space, equipping it with *systems capability* – that is, the ability to develop, build, and operate spacecraft – as well as the opening up of new markets. It is also about finding uses for space expertise in the contexts of civilian and military security. According to the German Aerospace Center statement, to accomplish its objectives, a balance needs to be maintained between the scientific- and application-based, or practical, uses of space, which in turn depends on maintaining Germany's technological independence and having unrestricted access to space transportation systems – and through them, to space.

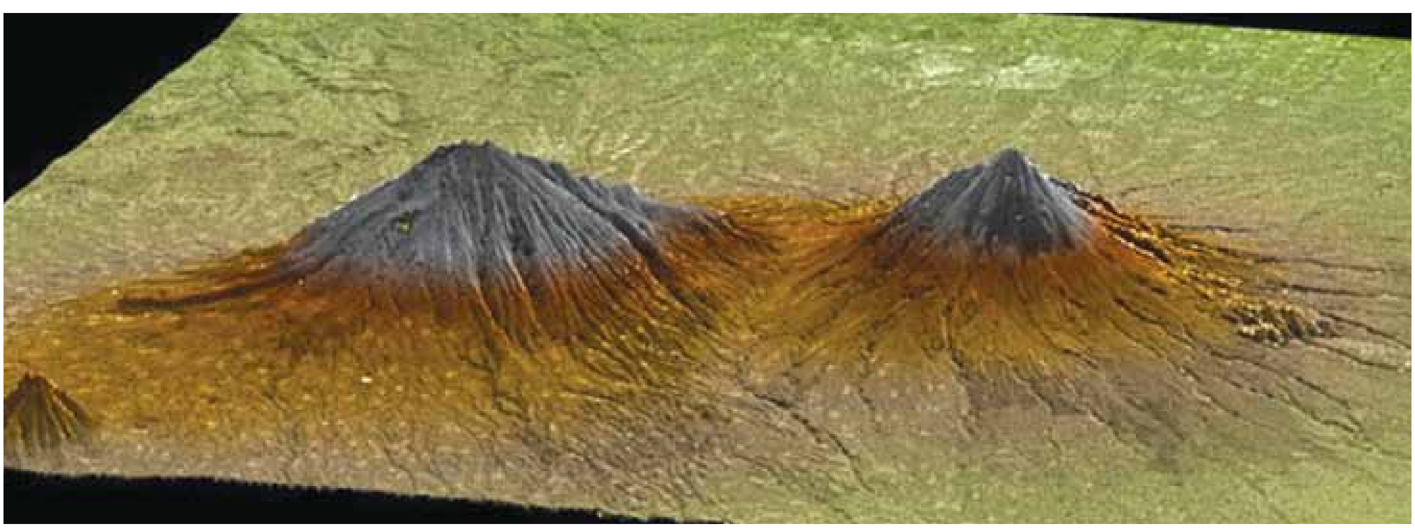

Figure 4 — Radar technology image of Merapi volcano (an active stratovolcano located on the border between Central Java and Yogyakarta, Indonesia) acquired by the TanDEM-X space satellite mission with the main objective of generating an accurate three-dimensional image of Earth. Image: German Aerospace Center (DLR)

Historic change occurs to atomic weights of ten elements

The atomic weights of ten elements listed on the Periodic Table of chemical elements will soon be adjusted to reflect a more precise reality.

The revised Periodic Table will express atomic weights of hydrogen, lithium, boron, carbon, nitrogen, oxygen, silicon, sulphur, chlorine, and thallium in a manner that will depict more accurately how these elements are found in nature. The atomic weights of these elements now will be expressed as intervals, having upper and lower bounds to reflect more accurately their variations in atomic weight.

Sulphur, for example, has a conventional atomic weight of 32.065. However, its actual atomic weight can be anywhere between 32.059 and 32.076, depending on where the element is found.

"In other words, knowing the atomic weight can be used to decode the origins and the history of a particular element in nature," said Dr. Michael Wieser, an associate professor at the University of Calgary, who serves as secretary of the International Union of Pure and Applied Chemistry's (IUPAC) Commission on Isotopic Abundances and Atomic Weights, the organization that oversees the evaluation and dissemination of atomic-weight values.

Elements with only one stable isotope do not exhibit variations in their atomic weights. For instance, the standard atomic weights for fluorine, aluminum, sodium, and gold are constant, and their values are known to better than six decimal places.

New star atlas

The *Cambridge Atlas of Herschel Objects,* written by James Mullaney, has just been released and it's magnificent – largely due to the celestial cartography of Wil Tirion! The maps in the new atlas are similar to those in the popular *Sky Atlas* (also created by Tirion) produced by *Sky and Telescope*; it is spiral-bound for use in the field and covers the entire sky, listing more than 2500 Herschel objects. The new volume is intended as a companion to an earlier work, *The Cambridge Double Star Atlas.* Both atlases are available from Cambridge University Press. ✶

Andrew I. Oakes is a long-time Unattached Member of RASC who lives in Courtice, Ontario.

Feature Articles
Articles de Fond

The Plaskett Lecture: Star Formation in the Perseus Molecular Cloud

Helen Kirk
NSERC PDF, Harvard Smithsonian Center for Astrophysics
hkirk@cfa.harvard.edu

Foreword

This article is based on my Plaskett Medal Lecture given at the annual CASCA meeting in Halifax, in May 2010. The Plaskett Medal is awarded to "the Ph.D. graduate from a Canadian university judged to have submitted the most outstanding doctoral thesis in astronomy or astrophysics in the preceding two calendar years." The lecture summarized my research during my thesis, as does this article. Contributions from Canadian facilities are highlighted where appropriate.

Abstract

Large-scale surveys of the Perseus molecular cloud have provided many clues as to the processes occurring during star formation. Here, analysis of both column density maps and kinematic data (maps and pointed data) are discussed and compared with predictions from simulations. Results include a column density threshold for the formation of dense star-forming cores and that the dense cores are quiescent within their local environment, while the molecular cloud as a whole has turbulent motions that are dominated by large-scale modes. Some of these results have already been used to constrain models of star formation, and the others can be included as future tests of the models. The next few years of star formation research promises to provide exciting advances to the field, particularly with the Gould Belt Legacy Surveys in progress at several facilities, including the James Clerk Maxwell Telescope (JCMT).

1. Introduction

Stars form within large complexes of gas and dust (at a ratio of ~100:1) known as molecular clouds. Molecular clouds were originally discovered as dark patches on the sky where no stars were visible. These "dark clouds" were first catalogued by Herschel (1785) and Barnard (1913); at the time, it was not known whether the dark patches represented an absence of stars or the obscuration of starlight by an unknown source. It took the advent of the radio telescope to solve the question – observations of the dark cloud in Orion revealed emission from the gas-phase molecule CO (carbon monoxide) (Wilson, Jefferts, & Penzias 1970), confirming the presence of material within them. CO is actually the second most abundant gas-phase species in a typical cloud. H_2 (molecular hydrogen) is the dominant species by a factor of at least 10^5. H_2 is not, however, observable under usual molecular-cloud conditions, so CO is often used as a proxy. Also found with H_2, CO, and other gas-phase molecules are dust grains, roughly micron-sized solid particles, which are responsible for the stellar obscuration.

We now know that stars typically form in these dark clouds, giant complexes of molecular gas and dust that span tens of parsecs (~30 light-years) and contain ~10,000 times the mass of material in our own Sun. Molecular clouds are hierarchically structured, and most of the mass (and area or volume) of the cloud is at low (column) densities, with only a small fraction in more condensed structures. The most compact structures are dense cores, the birthplace of stars. The large-scale clouds have densities around 100 particles per cm^3 and column densities of ~10^{21} particles per cm^2, while the associated dust obscures the background starlight by an A_V (visual extinction) of a few magnitudes. The cores have densities in excess of 10^5 cm^{-3} and column densities corresponding to tens or hundreds of A_V. To put this in perspective, even these dense cores are substantially more rarefied than the Earth's atmosphere!

The field of star-formation study is still young, with a mere 40 years of radio observations. There is still much to learn, despite the tremendous progress already made. This article focusses on observations connecting the dense cores to their larger environment. These new results provide a valuable way to learn about the processes that shape the formation and evolution of both the molecular cloud as a whole and the dense cores and stars forming within them.

A first look at a molecular cloud is puzzling. At the typical density and temperature for the cloud as a whole, thermal pressure can only prevent gravitational collapse for at most a few hundred solar masses worth of material. Molecular clouds contain hundreds of times more material than this, so how could they have formed that way without immediate collapse? There are two possible solutions. Gravitational collapse could be inhibited by additional physical processes. Alternatively, each cloud may not be a single well-defined entity – some parts may be collapsing while other parts are beginning to form, so that the "cloud" we observe stays visible for a much longer time period than any individual piece within it. Likely both of these are true to some extent. In this context, a variety of physical processes have been proposed for star formation. A few of the most popular ones include magnetic fields (*e.g.* Shu, Adams, & Lizano 1987), supersonic turbulent motions (*e.g.* MacLow & Klessen 2004), "global gravitation" (*e.g.* Burkert & Hartmann 2004), and "triggering" (*e.g.* Elmegreen 1998), all of which are briefly outlined below.

Magnetic fields primarily influence the behaviour of ionized atoms or molecules within the cloud, inhibiting their motion

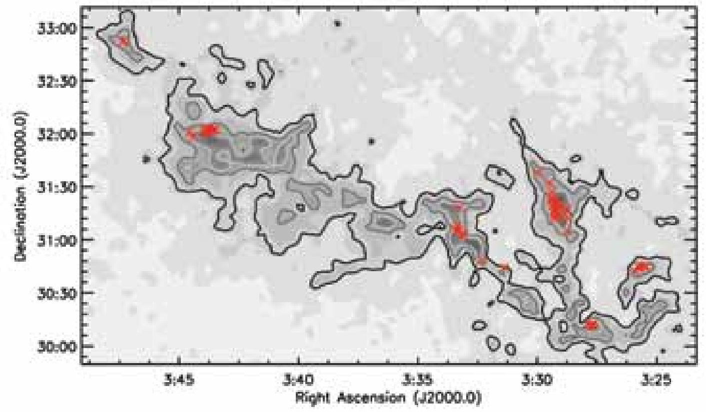

Figure 1 — An extinction map of the Perseus molecular cloud. Contours are shown at A_V of 3, 5, and 7 (dark to light lines). The locations of the dense cores identified are overlaid as red crosses. The SCUBA map in which the dense cores were identified spans a contiguous area covering beyond the black contour. Clearly, the dense cores tend to be found in regions of high extinction, despite the substantial coverage outside of these regions. Adapted from Kirk, Johnstone, & Di Francesco (2006).

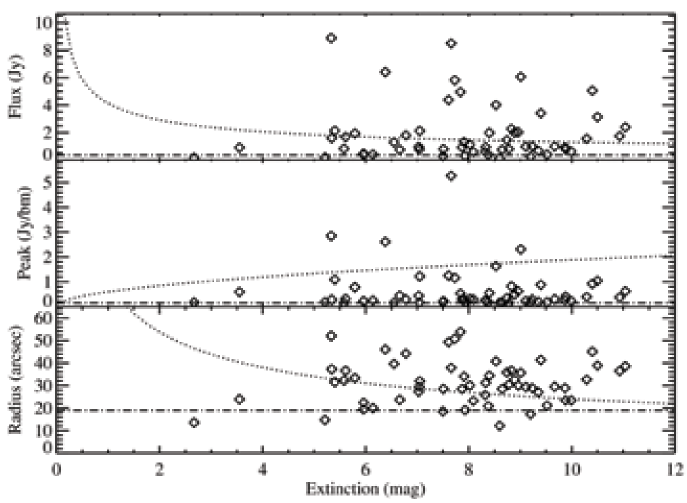

Figure 2 — Dense core properties as a function of the local extinction (large-scale column density) environment. From top to bottom: the total flux, peak flux, and radius of the dense cores. The diamonds show the observations, while the dotted line shows the behaviour of a Bonnor-Ebert sphere in varying pressured environments (low pressure corresponds to low column density or A_V). The dash-dotted line shows the approximate observational limits. Dense cores similar to those in regions of high extinction would be easily detectable at lower extinctions. Adapted from Kirk, Johnstone, & Di Francesco (2006).

perpendicular to the field lines. If the field is strong enough, then even neutral species have their motions reduced perpendicular to the field lines, slowed by frequent collisions with the motion-restricted ions. In this case, mass can only be concentrated into denser structures slowly, by the neutral species "drifting" past the ions in a process known as ambipolar diffusion. With a strong enough magnetic field, the timescale for gravitational collapse can be increased by a factor of ten or more.

Turbulent models come in a variety of forms, but in the most general picture, there are large-scale supersonic flows of material within molecular clouds. On the cloud-wide scale, these motions act to increase the effective temperature of the gas, allowing a larger amount of material to be stable to immediate gravitational collapse. Where the flows collide, the density is temporarily enhanced and can lead to the formation (and subsequent gravitational collapse) of dense cores. There are currently two main contending processes for how dense cores accrete their mass. The first is competitive accretion, in which a clustered distribution of protostellar "seeds" compete with each other for material within the larger cluster's gravitational potential. "Seeds" near the centre tend to gain more mass than the ones at the outskirts; interactions between the *seeds* play a major role in their evolution (*e.g.* Bonnell *et al.* 2001). The second scenario, monolithic collapse, posits that each dense core provides a self-sufficient reservoir for one or a small group of forming stars, so the mass that each star (or group) draws from is distinct; interactions between protostars are much less important (*e.g.* Tan, Krumholz, & McKee 2006).

The global gravitation model is related to the turbulent scenario above. The main distinction is that the turbulence is explicitly generated by gravity. Here, gravity acts on the large-scale structure of the cloud during its formation, inducing turbulent motions that are continuously driven by the large-scale evolution of the cloud. Material near the cloud edges where the curvature is higher tends to collapse first (in 2-D, finger-like regions coalesce before pancake-like regions), and the non-uniform motions induced by the evolution of the uneven "edges" of the molecular cloud percolate inwards, driving non-thermal motions in the cloud interior.

Triggering is a general term that encompasses a number of scenarios. Some triggering events start with a pre-existing stable structure, such as a dense core. The structure is then "triggered" to undergo gravitational collapse through an increase of pressure in its environment, typically caused by a nearby young massive (O or B) star "turning on" and increasing the radiation pressure in the local environment. Other triggering events can both create the structure and induce the subsequent evolution. An example of this is a supernova explosion – the shock wave from the explosion radiates outwards, sweeping up material in its path and collecting it into a ring or shell. Eventually, enough mass is collected that the ring/shell becomes gravitationally unstable and then fragments into a series of dense cores that could subsequently form stars.

These proposed processes have a major (and differing) impact on the large-scale evolution of molecular clouds, so determining their importance requires cloud-wide observations. Earlier observations focussed on regions where star formation was known to occur, but over the last several years, instrumentation has improved to the point where large-scale surveys are possible at a variety of wavelengths. Different wavelengths and different tracers are sensitive to complementary features of the star formation process; coordinated campaigns are vital for obtaining the full picture. With unbiased surveys, statistical measures of the properties of the clouds and the dense cores within them have the potential to rule out or place limits on the importance of the processes discussed above.

The Perseus molecular cloud is one of the best-studied molecular clouds to date, and I will highlight results from a coordinated survey of Perseus in which I was involved. Many of the observations were obtained under the auspices of the COMPLETE (COordinated Molecular Probe Line Extinction Thermal Emission) survey. COMPLETE was one of the earliest large multi-telescope, multi-wavelength star formation endeavours, focussing primarily on two nearby star-forming regions, Perseus and Ophiuchus (Goodman 2004, Ridge *et al.* 2006). Large-scale surveys are now underway at several telescopes (including the JCMT, *Spitzer*, and *Herschel*) covering many nearby molecular clouds, so the results and analyses discussed here offer a preview into the insights these new surveys will provide. Where possible, comparisons with predictions from the models described above are discussed. The majority of simulations to date focus on turbulence; few include magnetic fields, and only recently have predictions been made in the observational domain. Global gravitational simulations do not yet have the resolution for comparison with dense-core observations (see *e.g.* Heitsch *et al.* 2008), and so will not be discussed further here.

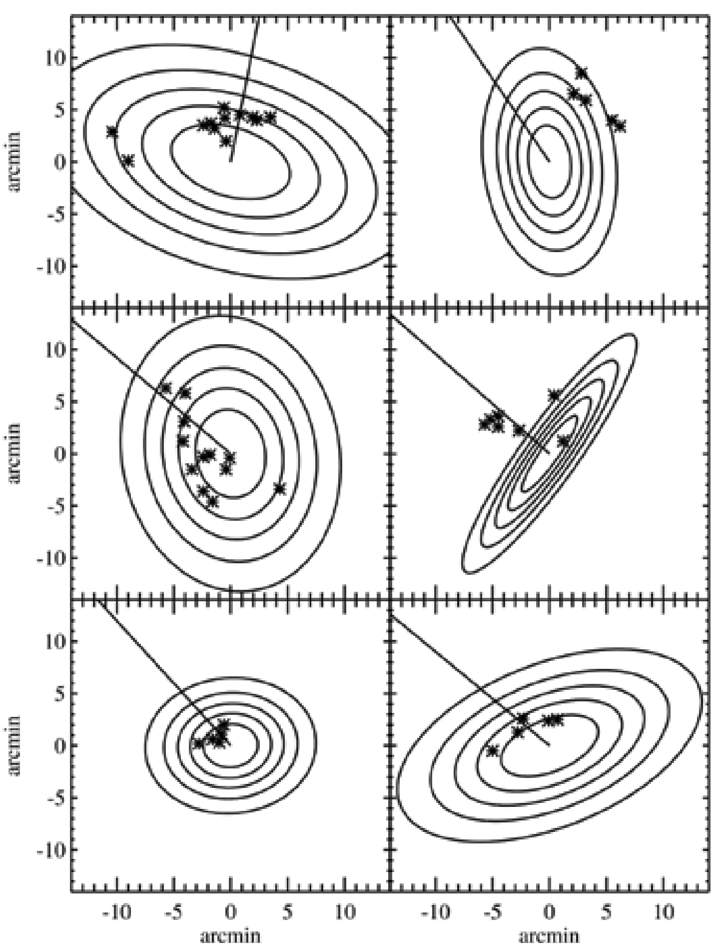

Figure 3 — A snapshot of the extinction peaks that harbour the most dense cores, showing the tendency of the dense cores to be offset from the peak of the extinction. The contours show a Gaussian model of the extinction, while the asterisks show the locations of the dense cores. The solid line points in the direction of 40 Per, which other work has suggested is triggering star formation in Perseus. There is reasonable qualitative agreement between the offset of the dense cores and the direction of 40 Per. Adapted from Kirk, Johnstone, & Di Francesco (2006).

2. Observations

The Perseus molecular cloud is a relatively nearby (250 pc/800 ly) star-forming region, and has properties mid-way between more extreme examples such as Taurus and Orion. Perseus shows more active and clustered star formation containing a mix of low and intermediate-mass stars, while Taurus is a very quiescent cloud that appears to be only forming a dispersed population of low-mass stars. Yet Perseus appears almost Taurus-like in comparison to the Orion molecular cloud, where a large population of high- and low-mass stars is forming dynamically in several large clusters. Across the galaxy, most stars appear to form in clusters (Lada & Lada 2003), and those in Perseus are more amenable to study than in Orion, as they are in smaller, sparser clusters with less source confusion. The entire Perseus cloud spans several square degrees on the sky, and has been mapped in a variety of tracers, some of which are described below.

2.1 Column Density Structure

The column density within molecular clouds is best measured using two complementary techniques. The large-scale column density structure is inferred using deep stellar catalogues. The dusty component of molecular clouds blocks (or extincts) the light from background stars, preferentially at shorter (bluer) wavelengths; areas with fewer and redder stars thus have a larger column density of material in front of them. One technique that has been applied to Perseus is NICER (Near Infrared Colour Excess - Revisited; Ridge *et al.* 2006). NICER (Lombardi & Alves 2001) uses observations at three near-infrared wavelengths to measure the stellar reddening and number density, taking advantage of the fact that most stars have similar intrinsic colours in the infrared and the extinction

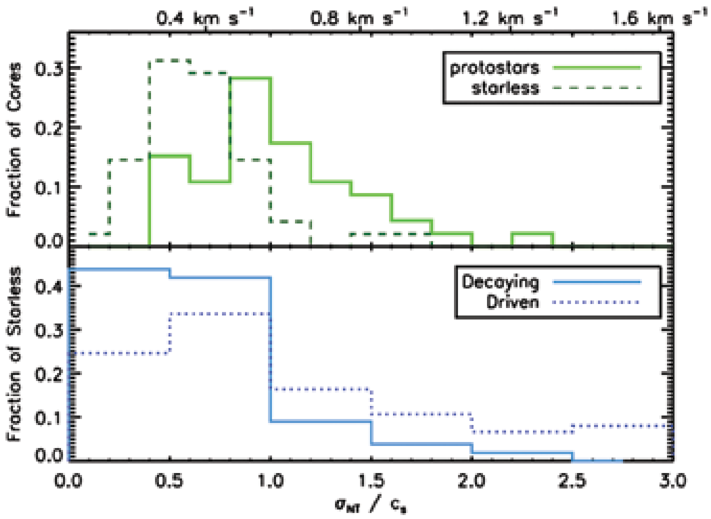

Figure 4 — The non-thermal motions within dense cores. The top panel shows the observed ratio of the non-thermal linewidth to the sound speed, split into starless and protostellar cores (dashed and solid lines). The bottom panel shows predictions for starless cores from two recent simulations by Offner et al. (2008), where the turbulence was allowed to decay (solid line) or was continuously driven (dotted line). The final bin for the driven turbulence simulation encompasses all data up to a ratio of 6. Clearly, the driven turbulence simulation is highly inconsistent with our observations of starless cores. Adapted from Kirk, Johnstone, & Tafalla (2007).

is less than at optical wavelengths. The derived dust column density from NICER or similar techniques is dependent only on the simple physics of dust grains scattering light – the temperature of the dust, for example, has no effect on the measure. The small-scale structure, however, cannot be probed with this method – the statistical measure of stellar reddening requires averaging over multiple stars; without very deep, targeted observations, a resolution of a few arcminutes is usually the best obtainable. At the distance of Perseus, dense cores are much smaller than this resolution, and cannot be probed with this method (for one region where "extinction mapping" has been successfully applied to the scale of cores, see Lombardi *et al.* 2006).

The small-scale column density distribution is measured by observing the thermal emission from the dust, typically using a submillimetre telescope, such as the James Clerk Maxwell Telescope (JCMT) in Hawaii, in which Canada is a major partner. The JCMT offers a resolution of 10 to 20 arcseconds, enough to (barely) resolve the dense cores. The thermal emission of dust can be used to estimate the column density, although care must be taken to consider the effect of temperature and varying dust-grain properties. The large-scale dust column density distribution cannot be measured by ground-based submillimetre facilities – the telescopes essentially make difference measures across the sky (necessitated by observing conditions), and so are insensitive to large-scale structure. In Perseus, the small-scale column density structure was mapped at the JCMT using SCUBA (Submillimetre Common-User Bolometer Array) primarily by Hatchell *et al.* (2005), with additional observations in Kirk, Johnstone, & Di Francesco (2006, hereafter Paper I). A slightly lower-resolution map was later made at the nearby Caltech Submillimeter Observatory (CSO) by Enoch *et al.* (2006).

2.1.1 Dense Core Extinction Threshold

In Paper I, we identified and analyzed the dense cores found in the JCMT SCUBA map, and then compared the locations of the dense cores within the large-scale cloud structure seen in the NICER extinction map. Figure 1 shows the extinction map, with contours at 3, 5, and 7 magnitudes of extinction and the locations of the dense cores overlaid as red crosses. Even at a quick glance, it is easy to see that the dense cores are not randomly distributed throughout the cloud – they lie only in regions of high extinction, despite the fact that the survey included a large area of the cloud at lower extinctions.

Modelling was required to test whether the lack of detection of cores at low extinction was due to observational sensitivity or whether it represented a true dearth of cores. Previous work (*e.g.* Johnstone *et al.* 2000) showed that dense cores can be roughly represented as Bonnor-Ebert (BE) spheres: isothermal, pressure-bounded spheres where self-gravity is balanced by thermal pressure. Using the BE sphere model, the observable properties of a dense core were predicted at different column densities (or extinctions), assuming that at lower column densities, the bounding pressure on the cores is smaller, as there is less overlying cloud material weighing on them. At lower column densities, therefore, the same core would be larger, less peaked, and able to support a larger amount of material against gravitational collapse. Figure 2 shows the predicted behaviour of core properties as a function of cloud extinction (dotted lines). The observed core properties are indicated by the diamonds, while the observational sensitivity is shown by the dash-dotted line. Clearly, dense cores similar to those found in the highest extinction parts of the cloud were detectable in the lower extinction parts; their absence indicates they were not able to form there.

A similar threshold for dense cores has also been found in several other star-forming regions, including Taurus (Onishi *et al.* 1998), Ophiuchus (Johnstone, Di Francesco, & Kirk 2004), and later Perseus through independent data and analysis (Enoch *et al.* 2006). A column density threshold for dense core formation was actually predicted by McKee (1989) for a magnetically dominated star-formation scenario. The basic premise of the paper was that dense cores can only coalesce in a reasonable amount of time in the very interior of molecular clouds. There, fewer ions exist to impede the formation of dense cores, as magnetic field lines inhibit the motion of ions across them. In the cloud exterior, the impinging UV radiation field ionizes too large a fraction of the cloud material, effectively hindering the motion of both ionized and non-ionized material. The extinction threshold predicted by McKee (1989), an A_V of 4 - 8 magnitudes, agrees with the observations. Simulations of turbulence-dominated or global gravity-dominated formation have not yet had sufficient dynamic range to test for this property.

2.1.2 Offset Core Locations

Upon a more thorough examination of Figure 1, a second property becomes apparent – while the dense cores were found in regions of higher column density, they appeared to be offset from the peaks of the extinction, in a preferential direction. Previous work by Walawender *et al.* (2004) showed that 40 Per, a nearby young B star, appeared to be shaping the cometary L1451 cloud (which lies below the bottom right-hand corner of Figure 1). The core offsets from the extinction peaks we found in Paper I were consistent with this triggering scenario. Figure 3 shows the six extinction peaks that harbour the densest cores. Contours indicate a Gaussian fit to the extinction, while the dense cores are shown as asterisks. The solid line points in the direction of 40 Per, showing that most of the offsets are in qualitative agreement with a triggered formation scenario.

2.2 Kinematics

Emission from gas-phase species within molecular clouds provides complementary information about the star-forming environment. Since clouds and cores are cold, often at temperatures around 15 K (-258 °C), the lowest few rotational energy level transitions in molecules (typically at radio or millimetre / submillimetre wavelengths) are best suited for detections. Since H_2 is often unobservable in this regime, trace species, such as CO, are commonly employed to study the cloud. Unlike the dust-emission observations, spectral observations provide velocity information allowing the measurement of both the bulk motion of the gas (through the wavelength of the centre of the emission line) and the level of motion between particles within the gas (through the width of the line). Chemistry and physical conditions affect which molecular transitions are observable, and are necessary to consider when interpreting observations. For example, CO and other carbon-bearing molecules tend to freeze out of the gas phase and onto dust grains at low temperatures and high densities, *i.e.* within dense cores (Tafalla *et al.* 2002). CO therefore provides an excellent tracer of the bulk cloud gas, but cannot be used to measure cores. Nitrogen-bearing molecules, such as NH_3 (ammonia) or N_2H^+ (diazenylium), on the other hand, trace the dense cores well, but not the bulk cloud gas, as their formation is inhibited by the presence of gas-phase CO. Different molecules therefore must be observed, depending on what is being studied.

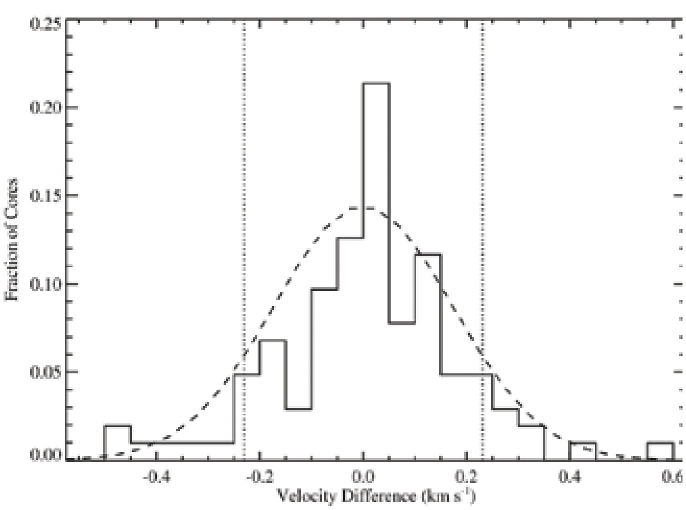

Figure 5 — The relative motion between the dense core and its surrounding envelope. The vertical dotted lines indicate the local sound speed, ~0.23 km s^{-1}. The dashed line shows a Gaussian fit to the histogram; the standard deviation of the observations is 0.17km s^{-1}. Adapted from Kirk, Johnstone, & Tafalla (2007).

In Kirk *et al.* (2007, hereafter Paper II), we surveyed the kinematics of the dense cores in Perseus with a pointed spectral survey of all of the dense cores identified in Paper I, as well as additional candidate dense cores, for a total of 157 targets. The survey included N_2H^+ (1-0) and $C^{18}O$ (2-1), which can be observed simultaneously at the IRAM 30-m telescope in Granada, Spain. N_2H^+ was used to probe the dense core, while $C^{18}O$ was used to probe the lower-density envelope surrounding the core; $C^{18}O$ is sensitive to a somewhat higher-density regime than its isotopologues ^{12}CO and ^{13}CO. Cores were classified as those that had already formed a young central source (protostars), and starless cores, based on a prior analysis that combined the SCUBA data with near- to mid-infrared observations from *Spitzer* (Jorgensen *et al.* 2007).

2.2.1 Thermally Dominated Cores

Consistent with previous work (*e.g.* Jijina, Myers, & Adams 1999), we found (Paper II) that the dense cores tended to have narrow linewidths, showing that the cores were thermally dominated. Assuming a temperature of 15 K (similar to that later measured in the Perseus cores in NH_3 by Rosolowsky *et al.* (2008), the non-thermal portion of the linewidth, σ_{nt}, was roughly half as large as the local sound speed, c_S, for the starless cores, and roughly equal for the cores that have already formed a protostar. Our survey was the first to make such a characterization for a homogenous population of dense cores in a single cloud; previous surveys typically used only a handful of cores from any given cloud. With these data, statistically significant comparisons with simulations and models could be made. Figure 4 shows a comparison of the ratio of σ_{nt} to c_S for the

Perseus dense cores versus simulated observations of two turbulence-dominated simulations tuned to have large-scale properties similar to Perseus (Offner *et al.* 2008). In one of the simulations, the turbulence was continuously driven on large scales, while in the other, it was allowed to decay as the simulation evolved. Our observations clearly rule out the driven simulation – there are far too many cores predicted that have large non-thermal motions. (We saw no cores with σ_{nt} / c_S above 1.8). The decaying turbulence scenario (solid light-blue line) is more consistent, although even there, too many dense cores are predicted at high σ_{nt} / c_S. The distribution of non-thermal motions within dense cores therefore provides an important avenue by which to test simulations.

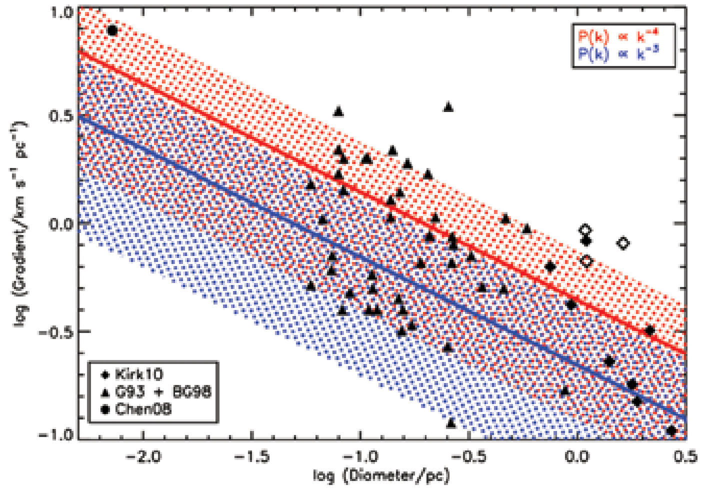

Figure 6 — The velocity gradient measured in ^{13}CO in each of the extinction regions versus the region size (diamonds). Regions where the measurement was more uncertain, due to incomplete coverage in ^{13}CO, are denoted by the open diamonds. Observations of NH3 cores from Goodman et al. *(1993) and Barranco & Goodman (1998) are shown by the triangles, and a high-resolution measurement of BHR-71 by Chen* et al. *(2008) is shown by the circle. The red and blue shading and lines show the zone and most likely values predicted for observations of regions dominated by large-scale modes of turbulence by Burkert & Bodenheimer (2000) for power spectra of P(k) α k^{-3} and k^{-4} respectively. Adapted from Kirk* et al. *(2010).*

2.2.2 Small Core-Envelope Motion

A second measure that provides a strong test for turbulent simulations is the motion between the dense core and its surrounding envelope. Walsh, Myers, & Burton (2004; hereafter WMB04) argued that turbulent simulations in which dense cores form via competitive accretion should show large relative motions between the dense cores and their envelopes. This was contrary to their observations of small motions between dense cores and their envelopes, although their survey focussed on dense cores in relatively isolated environments. Following WMB04, Ayliffe *et al.* (2007) made mock observations of a competitive accretion simulation, and found that they could reproduce the WMB04 results under certain circumstances, although in this case, the cores were not simultaneously thermally dominated. Unlike isolated star-forming environments, competitive accretion is expected to dominate in more clustered conditions, and our survey (Paper II) was the first to make similar measurements in this regime; see Figure 5. Similar to WMB04, we found that the core-envelope motion was small, usually less than the sound speed, with a standard deviation of 0.17 km s^{-1}, or ~75 percent of the sound speed. Debate continues as to whether competitive accretion simulations can match these observations. For example, in their mock observations of a competitive accretion simulation, Rundle *et al.* (2010) found small core-envelope motions with a standard deviation of 0.16 km s^{-1}, but also had core (N_2H^+) linewidths that were consistently non-thermal and *larger* than the corresponding envelope ($C^{18}O$) linewidths (see their Figure 17). Clearly more work is still needed to investigate these simulations.

2.2.3 Small Core-Core Motion

As a separate component of the COMPLETE survey, a full ^{13}CO(1-0) map of the Perseus cloud was made using the FCRAO (Ridge *et al.* 2006, Pineda, Caselli, & Goodman 2008). ^{13}CO is an excellent tracer of the bulk material within a molecular cloud, and so provides a complement to the KJT07 pointed dense-gas spectral survey. In Kirk *et al.* (2010, hereafter Paper III), we used the large-scale structures "extinction regions" identified in KJD06 to define sub-regions of Perseus to study. Most of the extinction regions corresponded to well-known star-forming regions such as IC348 and NGC1333. Within each extinction region, we measured the core-to-core velocity dispersion, as well as the total ^{13}CO velocity dispersion over the same region (calculated by summing all the ^{13}CO spectra). We found that the core-to-core velocity dispersions were roughly half as large as the ^{13}CO gas velocity dispersions. The number of cores in each extinction region was usually small, and the cores were often clustered within a small part of the region, however, neither of these effects appeared to be responsible for the factor of two difference in the velocity dispersions measured. Interpretation depends on the model adopted for the three-dimensional structure of the cloud (*i.e.* how much substructure there is along the line of sight), however, the measurement is straightforward to apply to simulations where the full cloud structure is known, and offers another way to test simulations.

2.2.4 Bulk Cloud Motions

Finally, in Paper III we analyzed the large-scale kinematic properties of the ^{13}CO gas. We measured the velocity gradient across each extinction region following the procedure outlined in Goodman *et al.* (1993). Gas following a turbulent power spectrum dominated by the largest-scale modes, as is usually assumed in turbulent simulations (*e.g.* Offner *et al.* 2008, Rundle *et al.* 2010), should follow a well-defined relationship between the velocity gradient and the size of the region for large-scale regions (Burkert & Bodenheimer 2000). Figure 6 shows the velocity gradient observed versus the diameter of each region (diamonds). The relationship and spread in observed values predicted for a turbulent power spectrum of $P \alpha k^{-4}$ and k^{-3} by Burkert & Bodenheimer (2000) are shown by the red and blue lines and shaded regions. The classical Kolmogorov incompressible turbulent power spectrum has a slope of -11/3, which lies between these values. For comparison, observations from Goodman *et al.* (1993) and Barranco & Goodman (1998) of NH_3 cores are shown by triangles, and a recent high-resolution observation of a dense core in the isolated Bok globule, BHR 71 from Chen *et al.* (2008) is shown by the circle. Clearly, the observations all follow the same trend and agree with the prediction for a turbulent power spectrum of roughly k^{-4}. Turbulence dominated by large modes therefore provides a good description of this cloud property.

3. Simulations

As can be seen from above, fully interpreting the observations usually requires comparison with predictions from simulations, which ideally are "observed" in a similar fashion as the actual observations. Few simulations yet incorporate magnetic fields (although one notable exception is the work of Nakamura & Li 2008), and most are run with a single set of initial conditions, due to computational limitations. The interaction between magnetic fields and turbulent motions and their combined effect on the evolution of the cloud is non-trivial, making parameter studies an important, but so far under-utilized approach. For that reason, we (Kirk, Johnstone, & Basu 2009) analyzed a suite of 21 simulations with varying initial magnetic-field strengths and levels of turbulence. These simulations were based on the setup described in Basu, Ciolek, & Wurster (2009), Ciolek & Basu (2006), and references therein. The simulations we analyzed had input Mach numbers ranging from 0 (thermal motions only) to 4 (dominated by turbulence) and an initial magnetic field ranging from very strong (μ_0 = 0.5) to very weak (μ_0 = 2), where μ_0 is the initial mass to magnetic-flux ratio. In order for the simulations to be able to run in a reasonable amount of time, they had a thin-sheet geometry, rather than being fully 3-D, however, they did include non-ideal MHD effects. Briefly, "observations" of these simulations showed that the distribution of core linewidths (2.2.1) was reproduced reasonably well in all of the simulations, however, the core-envelope motion (2.2.2) was more difficult – see Figure 7. None of the simulations we analyzed showed both small core-envelope motions and significant non-thermal velocity dispersion on the large scale (as observed in ^{13}CO for the extinction regions). This discrepancy with the observations may be due to the boundary conditions or geometry of the simulations, or indicate that additional physical processes are important. The analysis more importantly demonstrated that the core-envelope motion was an excellent discriminant for star- formation models, as we found it depends strongly on the initial conditions adopted in simulations.

4. Outlook for the Future

The observational benchmarks highlighted here can be used in conjunction with synthetic observations of numerical simulations in order to determine which processes dominate star formation both on the cloud-wide and dense core scale. Numerical simulations are ever improving to include more

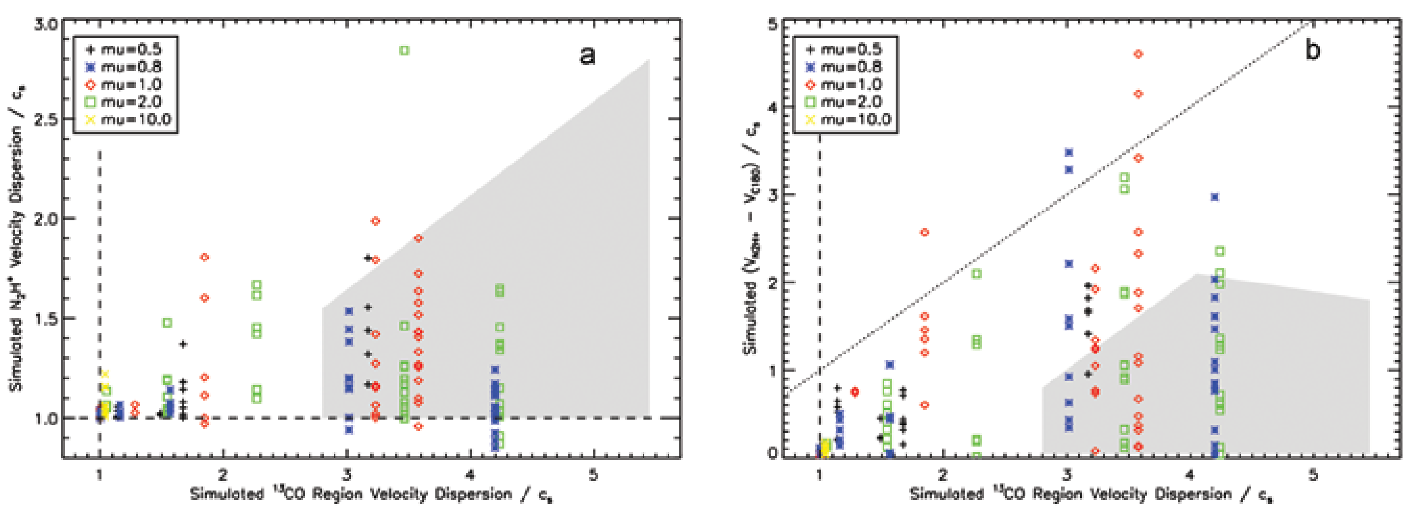

Figure 7 — A comparison between simulations and observations, with different initial magnetic-field strengths in the simulations denoted by different colours. The range spanned by the observations is shown by the grey shading. Left panel (a): velocity dispersion of N_2H^+ (the dense core gas) versus that of ^{13}CO (the cloud gas) across the entire extinction region or simulated box, in units of the sound speed. The dashed lines denote the sound speed, which is the minimum value expected. All simulations show a similar range in N_2H^+ velocity dispersion, independent of the region velocity dispersion, and the observations show a similar range. Right panel (b): The velocity difference between N_2H^+ and $C^{18}O$ (core and envelope gas in our observations) versus the ^{13}CO velocity dispersion of the extinction region or simulated box. The dotted line denotes a 1-1 correspondence. The observations show a much smaller range than the simulations at similar values of the ^{13}CO velocity dispersion. Adapted from Kirk, Johnstone, & Basu (2009).

physical processes, a finer level of detail, or span a larger parameter-space, and observations also face an exciting future. The strength of the observational measures presented here is the cloud-wide coverage in a variety of tracers, which has only recently become possible. So far, this type of analysis has not been applied to many clouds. That situation is changing, however, with Gould Belt Legacy Surveys (GLBS) in progress or completed at several telescopes, including *Spitzer*, *Herschel*, and the JCMT. The Gould Belt covers all nearby major star-forming regions, and hence, in the near future, measures similar to those discussed here can be made on a variety of molecular clouds. With this information, we will be able to understand the influence of environment on star-formation processes, and learn how typical Perseus is. Canadians have a strong involvement in the JCMT GBLS (Ward-Thompson *et al.* 2007), particularly the continuum-mapping component with the newly developed SCUBA-2 array. SCUBA-2 features a larger, more-sensitive detector than its predecessor, SCUBA, with an expected increase in mapping speed of well above an order of magnitude, making it ideal for large mapping projects. We are excited to see SCUBA-2 now in the commissioning phase at the JCMT.

Complementary to the developments in large-scale surveys are major advances for small-scale, high-resolution studies. The Atacama Large Millimetre Array (ALMA) is an array of more than 60 submillimetre dishes located in the Atacama desert at an altitude of 5000 m in Northern Chile. This facility represents a substantial increase in capabilities over current interferometric facilities, and will be operated by an international consortium including partners from North America, Europe, and East Asia. Canada is a major partner in the North American group and, through the instrument group at the Herzberg Institute for Astrophysics (in Victoria), is providing one of the key receivers for the dishes. ALMA will have the capability of studying structures at sub-arcsecond resolution for continuum or multiple spectral lines simultaneously. Many avenues of exploration will be opened by this new facility, including the fragmentation of dense cores (examining the formation of multiple-star systems) and the radial distribution of molecules within dense cores (tracing the chemical processes at work). Early science observations are expected to commence in less than a year.

5. Conclusions

The wealth of data covering the Perseus molecular cloud has allowed an unprecedented study of the cloud properties and the development of a series of statistically significant observational constraints on the processes shaping the evolution of the molecular cloud and dense cores within it. Several of these were highlighted here, summarizing the work in Kirk *et al.* (2006, 2007, 2009, 2010). A fuller, though likely still incomplete, list of studies based on recent Perseus survey data includes Curtis *et al.* (2010a, 2010b), Enoch *et al.* (2006), Foster *et al.* (2006, 2008, 2009), Goodman, Pineda, & Schnee (2009), Hatchell *et al.* (2005, 2007a, 2007b, 2008, 2009), Johnstone *et al.* (2010), Jorgensen *et al.* (2006, 2007, 2008), Kauffmann *et al.* (2010), Pineda *et al.* (2008, 2009, 2010), and Rosolowsky *et al.* (2008).

The results highlighted here include:

- Dense cores are only found in regions where the large-scale column density corresponds to a visual extinction of ~5 magnitude or higher. This is in agreement with predictions from a magnetically dominated formation scenario.
- Dense cores are thermally dominated, with only a small fraction (8 percent of starless cores) having a ratio of non-thermal to thermal motions greater than 1. This appears to rule out some models of turbulence-dominated formation.
- The motion between dense cores and their surrounding envelopes is small, typically less than the sound speed. There is debate over whether the competitive accretion scenario within a turbulence-dominated model can match this observation.
- The motion between dense cores within larger structures (extinction regions) is also small, roughly half of the total ^{13}CO gas velocity dispersion within the region. This measurement can be easily applied to future star-formation simulations.
- In each extinction region, the relationship between the ^{13}CO velocity gradient and dispersion is similar to that predicted for a turbulent power spectrum dominated by large-scale modes, with $P(k) \propto k^{-4}$.

The multi-wavelength coverage of Perseus has led to a richer understanding of this star-forming environment. Further advances will be made following upcoming surveys of other clouds. The next few years in star-formation research promise to provide substantial advances on the questions now posed, and will undoubtedly raise exciting new puzzles as well. Stay tuned!

Acknowledgements

HK thanks her many collaborators in the research highlighted here, in particular, her thesis advisor Doug Johnstone (HIA/UVic), as well as Shantanu Basu (UWO), James Di Francesco (HIA/UVic), Alyssa Goodman (CfA), Jaime Pineda (Manchester), and Mario Tafalla (OAN). HK also thanks Doug Johnstone for providing useful suggestions about this manuscript. HK is supported by a Natural Sciences and Engineering Research Council of Canada Postdoctoral Fellowship, with additional support from the Smithsonian Astrophysical Observatory. She gratefully acknowledges support from NSERC, NRC, and University of Victoria fellowships during her thesis research. ✶

References

Ayliffe, B.A., Langdon, J.C., Cohl, H.S., & Bate, M.R. (2007). On the relative motions of dense cores and envelopes in star-forming molecular clouds. *MNRAS, 374,* (4), 1198-1206

Barnard, E.E. (1913). Dark regions in the sky suggesting an obscuration of light. *ApJ*, *38*, 496-501

Barranco, J.A. & Goodman, A.A. (1998). Coherent Dense Cores I. NH3 Observations. *ApJ*, *504*, 207-222

Basu, S., Ciolek, G.E., & Wurster, J. (2009). Nonlinear evolution of gravitational fragmentation regulated by magnetic fields and ambipolar diffusion. *New Astronomy, 14* (3), 221-237

Bonnell, I.A., Clarke, C.J., Bate, M.R., & Pringle, J.E. (2001). Competitive accretion in embedded stellar clusters. *MNRAS,* 323 (4), 785-794

Burkert, A. & Bodenheimer, P. (2000). Turbulent Molecular Cloud Cores: Rotational Properties. *ApJ, 543* (2), 822-830

Burkert, A., & Hartmann, L. (2004). Collapse and Fragmentation in Finite Sheets. *ApJ, 616* (1), 288-300

Chen, X., Laundhardt, R., Bourke, T.L., Henning, T., & Barnes, P.J. (2008). ATCA and Spitzer Observations of the Binary Protostellar Systems CG 30 and BHR 71. *ApJ, 683* (2), 862-875

Ciolek, G.E. & Basu, S. (2006). Formation and Collapse of Nonaxisymmetric Protostellar Cores in Planar Magnetic Interstellar Clouds: Formulation of the Problem and Linear Analysis. *ApJ, 652* (1), 442-457

Curtis, E.I., Richer, J.A., & Buckle, J.V. (2010a). A submillimetre survey of the kinematics of the Perseus molecular cloud -I. Data. *MNRAS, 401* (1), 455-472

Curtis, E.I., Richer, J.S., Swift, J.J., Williams, J.P. (2010b). A submillimetre survey of the kinematics of the Perseus molecular cloud - II. Molecular outflows. *MNRAS, 408* (3), 1516-1539

Enoch, M.L. *et al.* (2006). Bolocam Survey for 1.1 mm Dust Continuum Emission in the c2d Legacy Clouds. I. Perseus. *ApJ, 638* (1), 293-313

Elmegreen, B.G. (1998). Observations and Theory of Dynamical Triggers for Star Formation. In C.E. Woodward, J.M. Shull, and H.A. Thronson, Jr. (Eds.) *Origins, ASP Conference Series, Vol. 148,* (pp. 150-183)

Foster, J.B. & Goodman, A.A. (2006). Cloudshine: New Light on Dark Clouds. *ApJ, 636* (2), L105-L108

Foster, J.B., Roman-Zuniga, C.G., Goodman, A.A., Lada, E.A., & Alves, J. (2008). Hunting Galaxies to (and for) Extinction. *ApJ, 674* (2), 831-845

Foster, J.B., Rosolowsky, E.W., Kauffmann, J., Pineda. J.E., Borkin, M., Caselli, P., Myers, P.C., & Goodman, A.A. (2009). Dense Cores in Perseus: The Influence of Stellar Content and Cluster Environment. *ApJ, 696* (1), 298-319

Goodman, A.A., Benson, P.J., Fuller, G.A., & Myers, P.C. (1998). Dense cores in dark clouds. VIII - Velocity gradients. *ApJ, 406* (2), 528-547

Goodman, A.A. (2004). The COMPLETE Survey of Star-Forming Regions on its Second Birthday In D. Johnstone, F.C. Adams, D.N.C. Lin, D.A. Neufeld, and E.C. Ostriker (Eds.), *Star Formation in the Interstellar Medium: In Honor of David Hollenbach, Chris McKee and Frank Shu* (Vol 323, pp171-179). San Francisco, CA: Astronomical Society of the Pacific

Goodman, A.A., Pineda, J.E., & Schnee, S.L. (2009). The "True" Column Density Distribution in Star-Forming Molecular Clouds. *ApJ, 692* (1), 91-103

Hatchell, J., Richer, J.S., Fuller, G.A., Qualtrough, C.J., Ladd, E.F., & Chandler, C.J. (2005). Star formation in Perseus. Clusters, filaments and the conditions for star formation. *A&A, 440* (1), 151-161

Hatchell, J., Fuller, G.A., Richer, J.A., Harries, T.J., & Ladd, E.F. (2007a). Star formation in Perseus II. SEDs, classification and lifetimes. *A&A, 468* (3), 1009-1024

Hatchell, J., Fuller, G.A., & Richer, J.S. (2007b). Star formation in Perseus. III. Outflows. *A&A, 472* (1), 187-198

Hatchell, J. & Fuller, G.A. (2008). Star formation in Perseus. IV. Mass-dependent evolution of dense cores. *A&A, 482* (3), 855-863

Hatchell, J. & Dunham, M.M. (2009). Star formation in Perseus. V. Outflows detected by HARP. *A&A, 502* (1), 139-153

Heitsch, F., Hartmann L.W., Slyz, A.D., Devriendt, J.E.G., Burkert, A. (2008). Cooling, Gravity, and Geometry: Flow-driven Massive Core Formation. *ApJ, 674* (1), 316-328

Herschel, W. (1785). On the Construction of the Heavens. *Philosophical Transactions of the Royal Society of London*, *75*, 213-266

Jijina, J., Myers, P.C., & Adams, F.C. (1999). Dense Cores Mapped in Ammonia: A Database. *ApJS, 125* (1), 161-236

Johnstone, D., Wilson, C.D., Moriarty-Schieven, G., Joncas, G., Smith, G., Gregersen, E., Fich, M. (2000). Large-Area Mapping at 850 Microns. II. Analysis of the Clump Distribution in the Rho Ophiuchi Molecular Cloud. *ApJ, 545* (1), 327-339

Johnstone, D., Di Francesco, J., & Kirk, H. (2004). An Extinction Threshold for Protostellar Cores in Ophiuchus. *ApJ, 611* (1), L45-L48

Johnstone, D., Rosolowsky, E., Tafalla, M., & Kirk, H. (2007). Dense Gas Tracers in Perseus: Relating the N2H+, NH3, and Dust Continuum Properties of Pre- and Protostellar Cores. *ApJ, 711* (2), 655-670

Jorgensen, J.K. *et al.* (2006). The Spitzer c2d Survey of Large, Nearby, Interstellar Clouds. III. Perseus Observed with IRAC. *ApJ, 645* (2), 1246-1263

Jorgensen, J.K., Johnstone, D., Kirk, H., & Myers, P.C. (2007). Current Star Formation in the Perseus Molecular Cloud: Constraints from Unbiased Submillimeter and Mid-Infrared Surveys. *ApJ, 656* (1), 293-305

Jorgensen, J.K., Johnstone, D., Kirk, H., Myers, P.C., Allen, L.E., Shirley, Y.L. (2008). Current Star Formation in the Ophiuchus and Perseus Molecular Clouds: Constraints and Comparisons from Unbiased Submillimeter and Mid-Infrared Surveys. II. *ApJ, 683* (2), 822-843

Kauffmann, J., Pillai, T., Shetty, R., Myers, P.C., Goodman, A.A. (2010). The Mass-Size Relation from Clouds to Cores. I. A New Probe of Structure in Molecular Clouds. *ApJ, 712* (2), 1137-1146

Kirk, H., Johnstone, D., & Di Francesco, J. (2006). The Large- and Small-Scale Structures of Dust in the Star-forming Perseus Molecular Cloud. *ApJ, 646* (2), 1009-1023

Kirk, H., Johnstone, D., & Tafalla, M. (2007). Dynamics of Dense Cores in the Perseus Molecular Cloud. *ApJ, 668* (2), 1042-1063

Kirk, H., Johnstone, D., & Basu, S. (2009). The Interplay of Turbulence and Magnetic Fields in Star-Forming Regions: Simulations and Observations. *ApJ, 699* (2), 1433-1453

Kirk, H., Pineda, J.E., Johnstone, D., Goodman, A.A. (2010). The Dynamics of Dense Cores in the Perseus Molecular Cloud. II. The Relationship Between Dense Cores and the Cloud. *ApJ, 723,* (1), 457-475

Lada, C.J., & Lada, E.A. (2003). Embedded Clusters in Molecular Clouds. *ARA&A, 41,* 57-115

Lombardi, M. & Alves, J. (2001). Mapping the interstellar dust with near-infrared observations: An optimized multi-band technique. *A&A, 377,* 1023-1034

Lombardi, M., Alves, J., & Lada, C.J. (2006). 2MASS wide field extinction maps. I. The Pipe nebula. *A&A, 454* (3), 781-796

McKee, C. (1989). Photoionization-regulated star formation and the structure of molecular clouds. *ApJ, 345,* 782-801

MacLow, M-M. & Klessen, R.S. (2004). Control of star formation by supersonic turbulence. *Reviews of Modern Physics, 76* (1), 125-194

Nakamura, F. & Li, Z-Y. (2008). Magnetically Regulated Star Formation in Three Dimensions: The Case of the Taurus Molecular Cloud Complex. *ApJ, 687* (1), 354-375

Offner, S.S.R., Krumholz, M.R., Klein, R.I., McKee, C.E. (2008). The Kinematics of Molecular Cloud Cores in the Presence of Driven and Decaying Turbulence: Comparisons with Observations. *ApJ, 136* (1), 404-420

Onishi, T., Mizuno, A., Kawamura, H.O., & Fukui, Y. (1998). A C18O Survey of Dense Cloud Cores in Taurus: Star Formation. *ApJ, 502* (1), 296-314

Pineda, J.E., Caselli, P., & Goodman, A.A. (2008). CO Isotopologues in the Perseus Molecular Cloud Complex: the X-factor and Regional Variations. *ApJ, 679* (1), 481-496

Pineda, J.E., Rosolowsky, E.W., Goodman, A.A. (2009). The Perils of Clumpfind: The Mass Spectrum of Substructures in Molecular Clouds. *ApJ, 699* (2) L134-L138

Pineda, J.E., Goodman, A.A., Arce, H.G., Caselli, P., Foster, J.B., Myers, P.C., & Rosolowsky, E.W. (2010). Direct Observation of a Sharp Transition to Coherence in Dense Cores. *ApJ, 721* (1), L116-L121

Ridge, N.A., Di Francesco, J., Kirk, H., Li, D., Goodman, A.A., Alves, J.F., Arce, H.G., Borkin, M.A., Caselli, P., Foster, J.B., Heyer, M.H., Johnstone, D., Kosslyn, D.A., Lombardi, M., Pineda, J.E., Schnee, S.L., & Tafalla, M. (2006). The COMPLETE Survey of Star-Forming Regions: Phase I Data. *ApJ, 131,* (6) 2921-2933

Rosolowsky, E.W., Pineda, J.E., Foster, J.B., Borkin, M.A., Kauffman, J., Caselli, P., Myers, P.C., & Goodman, A.A. (2008). An Ammonia Spectral Atlas of Dense Cores in Perseus. *ApJS, 175* (2), 509-521

Rundle, D., Harries, T.J., Acreman, D.M., & Bate, M.R. (2010). Three-dimensional molecular line transfer: a simulated star-forming region. *MNRAS, 407* (2), 986-1002

Shu, F.H., Adams, F., Lizano, S. (1987). Star formation in molecular clouds - Observation and theory. *ARA&A, 25*, 23-81

Tan, J.C., Krumholz, M.R., & McKee, C.F. (2006). Equilibrium Star Cluster Formation. *ApJ, 641* (2), L121-L124

Tafalla, M., Myers, P.C., Caselli, P., Walmsley, C.M., & Comito, C. (2002). Systematic Molecular Differentiation in Starless Cores. *ApJ, 569,* (2), 815-835

Walawender, J., Bally, J., Reipurth, B., & Aspin, C. (2004). Deep Imaging Surveys of Star-Forming Clouds II. A New Giant Herbig-Haro Flow in L1451. *AJ, 127* (5), 2809-2816

Walsh, A.J., Myers, P.C., & Burton, M.G. (2004). Star Formation on the Move? *ApJ, 614* (1), 194-202

Ward-Thompson, D. *et al.* (2007). The James Clerk Maxwell Telescope Legacy Survey of Nearby Star-forming Regions in the Gould Belt. *PASP, 119* (858), 855-870

Wilson, R.Q., Jefferts, K.B., & Penzias, A.A. (1970). Carbon Monoxide in the Orion Nebula. *ApJ, 161,* L43

Challenging Einstein: Gravitational Lensing as a Test of General Relativity

Jordan Friesen, Adam Rogers, & Jason D. Fiege
Department of Physics and Astronomy, The University of Manitoba, Winnipeg, Manitoba, Canada R3T 2N2

Abstract

The phenomenon of gravitational lensing, the deflection of light by gravitational fields, has grown from curiosity into the realm of precision science. In fact, this effect was one of the main methods initially used to verify Einstein's theory of general relativity. In this paper, we discuss the historical development of the field and simulations of optical solar-eclipse observations that illustrate the difficulty of the method. Our simulations predict the change in the position of the stars in the upcoming 2012 eclipse that will be visible during totality from Cairns, Australia. We have found also that the largest deflection angle of background starlight in the near future will occur during the 2019 eclipse, marking 100 years since Eddington's initial observations. This will provide an interesting opportunity to potentially reproduce Eddington's observations on the centennial anniversary of his historic eclipse expedition.

1. Introduction

The first mathematical description of gravity was provided by Sir Isaac Newton in 1687. Newton's law of universal gravitation describes the force of gravity F acting between two objects having mass M and m, separated by a distance between their centres r. This force is then written:

$$F = \frac{GMm}{r^2} \qquad (1)$$

where G is a universal constant. By using this simple equation, Newton was able to predict the orbits of the planets and the dynamical behaviour of the Solar System with great success. However, Newton was a man of many interests, including optics. He believed that light was made up of infinitessimal material bodies, each of which was presumed to have a tiny mass. It seemed natural for Newton to be the first to ask: Is it possible for the gravitational force to act on light? If this were the case, it would appear to a distant observer that a light ray would bend around a massive object.

The first quantitative description of light deflection due to gravitation was carried out by the German physicist Johann von Soldner in 1804 (Soldner 1804). Soldner used Newton's law of universal gravitation, Equation 1, and found the amount by which light should be deflected if the path of the ray just grazed the surface of the Sun. The deflection angle at the edge of the Sun, denoted α, was calculated to be α = 0.84 arcsec.

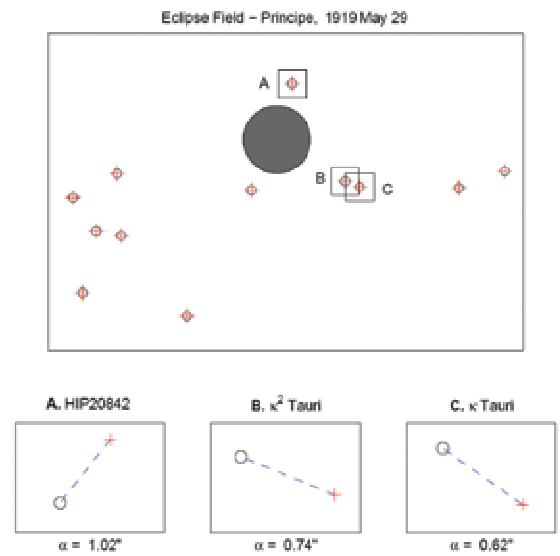

Figure 1, top — Configuration of stars during the 1919 eclipse as seen from Principe, Africa. Circles represent the true positions of background stars, and image positions are represented by a cross. Bottom: The lower set of figures represents close-up views of the stars indicated in the top figure.

This calculation would remain a mere curiosity until a century later.

In 1905, Albert Einstein described the theory of special relativity (Einstein 1905). This theory forever changed our view of the Universe, describing space and time unified in one four-dimensional entity: space-time. Using this framework, Einstein was able to show that the laws of electromagnetism – the description of electricity, magnetism, and light itself – require that the speed of light be constant for all observers. This has some shocking consequences: time and distance were no longer constant for all observers. Rather, it is the state of relative motion of two observers that determines the passage of time and distances measured between them. Since the speed of light is so central to his theory and to the mechanics of space-time, Einstein calculated the effect that the Sun would have on a light ray. In this first calculation, Einstein used an as-yet incomplete description of space-time to model the effect. Though Soldner's work was unknown to him at this time, Einstein's initial calculation agreed with Soldner's result.

Following his initial successes, Einstein began to work on a more complete description of space-time, known as general relativity (GR; Einstein (1915)). This theory was Einstein's masterwork and was published in 1915. Once again, Einstein demolished commonly accepted notions of the Universe. In GR, gravity is a consequence of space-time *curving* around a massive object.

GR is a remarkable theory because it includes all of the results of special relativity (found when space-time is not curved at all) and Newton's law of gravitation (found when space-time is

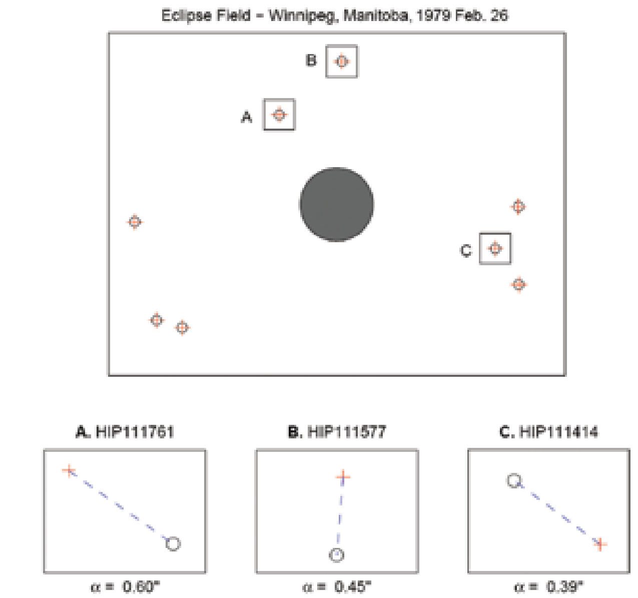

Figure 2 — Configuration of stars during the 1979 eclipse as seen from Winnipeg, Manitoba, Canada. Note the small size of the deflection angles compared to the 1919 eclipse.

only gently curved, as on the surface of the Earth and far from the Sun). This means that all of the successes of both Einstein and Newton's former works are contained in GR. The theory also makes some predictions that are far from our everyday experience, describing the physics of black holes, the expanding Universe, and the Big Bang.

Given these strange predictions, how did physicists convince themselves that Einstein's theory was correct?

2. Testing General Relativity

Once his description of space-time was complete, Einstein returned to the question of light deflection due to gravity. This time, Einstein used the full-blown theory of GR, taking into account the space-time curvature around the Sun, to calculate the deflection angle α. Surprisingly, he found that the solution was twice Soldner's previously calculated result.

To describe the gravitational-lens effect quantitatively, let us define the deflected position of a star by an angle θ. This is the position of the star as it would be seen under the influence of the gravitational-lens effect. Let the distance between the Earth and Sun be D_d. The deflection angle of a light ray produced by a point mass M as a function of deflected position θ is then:

$$\alpha(\theta) = \frac{4GM}{c^2 D_d \theta} \qquad (2)$$

using the mass of the Sun M, the solar radius $r = D_d\theta$, the speed of light c and converting to arcsecond units (1° = 3600″), we find that the deflection angle at the limb of the Sun is α = 1.75″. The extra factor of 2 enters into the complete description because of the space-time curvature effects, and was absent in Einstein's previous estimate.

In fact, we can go a step further and relate the undeflected *(true)* angular position of a star in the absence of the lens effect, β, with the deflected position θ. The relationship between these two quantities is called the thin-lens equation:

$$\beta = \theta - \alpha(\theta) \qquad (3)$$

with $\alpha(\theta)$ given by equation 2. Inserting this expression into equation 3 and solving for θ, we find a quadratic equation

$$\theta^2 - \beta\theta - \frac{4GM}{c^2 D_d} = 0 \qquad (4)$$

that can then be solved by application of the quadratic formula:

$$\theta_\pm = \frac{1}{2}\left(\beta \pm \sqrt{\beta^2 - \frac{16GM}{c^2 D_d}}\right) \qquad (5)$$

This expression gives the resulting deflected position of the star as a function of undeflected position β. Note that the equation has two solutions, θ_+ and θ_-. In the case of lensing by the Sun, one solution (θ_-) is near the centre of the Sun's disk and cannot be observed. Therefore, during an eclipse, the position of a background star will be deflected to a new position θ_+. Though the magnitude of the deflection is small, Einstein knew that if this *gravitational-lensing* effect were observed by the amount he calculated, it could be used to validate his theory of GR along with all of its exotic predictions. However, the measurements are difficult in practice for a variety of reasons.

In order to observe gravitational lensing of light by the mass of the Sun, it is necessary to see the background stars near the Sun. This can be done by observing the sky during a solar eclipse. With the Moon occulting the Sun's disk at totality, enough sunlight is blocked so that stars are visible; the stars nearest the Sun are deflected the most severely. The separation between the stars can then be measured in the sky when the Sun is absent, and the difference can be attributed to the gravitational-lens effect. From Equation 2, we can see that the deflection angle decreases as $1/\theta$ as we move away from the Sun. The maximum deflection possible is therefore 1.75 arcseconds, but smaller deflections are observed in practice, since observations require bright stars to be present near the limb of the Sun during totality. Furthermore, the observations have to be made in the path of totality, so an expedition would usually have to be mounted and astronomical equipment moved into place at the site.

The first observer to undertake the challenge of testing GR was the British astronomer Arthur Eddington. Eddington, along with the Astronomer Royal, Frank Dyson, planned an expedition to sites in Africa (Principe) and Brazil (Sobral), to observe the 1919 eclipse (Dyson, Eddington, and Davidson 1919). The expedition was beset by difficulties. While there, one of the telescopes malfunctioned due to the heat and produced only blurry images (Almassi 2009). Furthermore, the Principe site was shrouded in cloud cover for hours before totality. The clouds only parted a half hour before the critical moment, allowing the team to scramble to produce reliable observations (Kennefick 2007).

In order to illustrate the difficulty of these observations, we have produced graphics using the *MATLAB* programming language (www.mathworks.com) that simulates the positions of the stars Eddington observed during the eclipse. We found the dates and locations of totality of solar eclipses using the NASA Eclipse Web site (http://eclipse.gsfc.nasa.gov). We then find the undeflected positions, β, of the background stars near the Sun at this time and location on Earth using planetarium software *(Starry Night Pro+ version 6.0)*. Using these positions in equation 5, we calculate the resulting positions θ_+ as they would appear under the effect of gravitational lensing by the Sun.

Though the value 1.75″ is often used casually, it is difficult to comprehend how tiny an angle this truly is in practice. To demonstrate this, consider Figure 1. The large upper panel shows the stars' undeviated position and observed deflected position under the gravitational-lens effect, which appears at first glance non-existent! However, a closer inspection of the stars (lower panels) shows that there is actually a deflection of each of these stars, though their deviations are extremely small. Nevertheless Eddington's 1919 expedition managed to find a solar deflection angle of α = 1.61″± 0:30 at Principe and α = 1.98″ ± 0.12 at Sobral, versus the GR value of 1.75″. These observations favour a large deflection angle, as found from GR, rather than half this value, which would have supported the Newtonian value derived by Soldner. Eddington's observations validated GR and forever burned Einstein's name into the public consciousness.

There remains a significant amount of controversy over Eddington's results. The plates that were discarded from the initial analysis were obtained with the 13″ Astrographic telescope of the Royal Observatory at Sobral. These plates were said to show a deflection that was much smaller than Einstein predicted, α = 0.93″. This deflection angle is more in line with the Newtonian prediction than the prediction of GR. If these plates had been included in the original analysis, the measurements would have significantly reduced Eddington's observed value of the deflection angle. The problem with these plates is that the telescope focus seems to have changed significantly between reference image and eclipse observation due to the heat on-site and was therefore discounted. Since Eddington's observations were a strong piece of evidence in support of Einstein's theory, this would have been a serious setback for GR. However, re-analysis of the surviving Sobral plates in 1979 (Harvey 1979) has shown that, when properly referenced using modern means, the Sobral plates give a result consistent with the other observations, yielding a revised deflection angle of α = 1.52″ ± 0.34.

3. Historical Development

Since Eddington's historical expedition, the observation of the gravitational-lens effect has been repeated a number of times. Efforts were made to observe subsequent eclipses in 1922, 1929, two expeditions in 1936, 1947, 1952, and 1973 (Will 1993). Subsequent efforts to measure the effect provided similar results with little improvement. The measured values of the deflection angle lie typically between 0.75 to 1.5 times Einstein's predicted value. Even the 1973 expedition achieved only a modest accuracy of 0.95 ± 0.11 times the predicted value.

Extremely high accuracy is required to experimentally validate GR by the deflection of starlight during an eclipse, and the required accuracy is difficult to achieve even with modern instrumentation. In fact, the 1973 eclipse is the last time the measurement was attempted optically. Astronomers had found a better way to perform these kinds of observations using the fact that GR predicts that gravitational lensing affects all wavelengths equally.

As a result, much more accurate measurement of the lensing effect can be made using radio telescopes and quasars rather than observations of stars in the visible spectrum. Quasars are cosmologically distant active galaxies. These galaxies are highly luminous (approximately 100 times that of the total light of average galaxies like the Milky Way), which allows them to be seen from cosmological distances. About one in ten quasars is also radio-loud and can be observed in daylight at radio wavelengths; thus a solar eclipse is not required. These radio-loud quasars provide excellent targets for verifying the lensing effect, provided that several of them can be observed simultaneously near the limb of the Sun. In fact, this is exactly what was found with the quasar pair 3C 273 and 3C 279. Every October, the Sun passes this pair of quasars in the sky, and the separation between them can be readily measured using radio interferometry (Will 1993). By making a series of measurements, the deflection

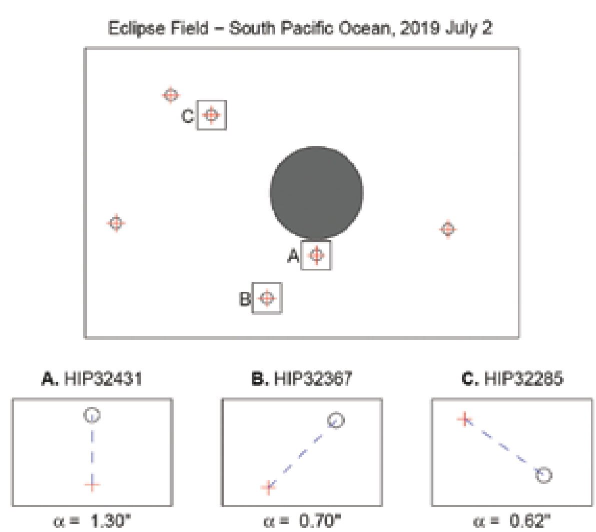

Figure 3 — Configuration of stars during the 2012 eclipse as seen from Cairns, Australia.

angle as a function of distance from the Sun can be determined, and the results have shown that a light ray passing near the limb of the Sun behaves as GR predicts. These observations were carried out annually between 1969 and 1975, and the uncertainty in the measurements was gradually reduced from the 20-percent error found in optical-light-deflection measurements to 0.01 percent using lensed groups of quasars (Fomalont and Sramek 1975). Over time, the technique was improved to μarcsecond – a millionth of an arcsecond – accuracy (Robertson, Carter, and Dillinger 1991). In fact, due to these high-precision methods, the gravitational lensing of background radio sources by the planet Jupiter was first carried out in 1991. Though the observations only had a precision of 50 percent, this result is impressive because the lensing effect at the limb of Jupiter comprises an angle of only 17 milliarcseconds, a hundred times smaller than that of the Sun (Treuhaft and Lowe 1991).

3.1. Gravitational Lensing Occurs on Many Scales

After Eddington's observations were made public, Einstein began to consider other gravitational-lens configurations. Einstein (1936) showed that the perfect alignment of background and foreground stars along the line of sight would produce an image that would appear to a distant observer as a full ring. As the background star is increasingly offset from the line of sight, an observer would see the image as a partial arc. This circular image is now known as an Einstein ring, the radius of which can be found by setting $\beta = 0$ in equation 5. Since he considered effects only from individual stars, Einstein thought that these exotic imaging effects due to gravitational lensing would remain unobserved. However, only a year later, Fritz Zwicky (1937) postulated that a far more dramatic gravitational-lensing effect could be observed when a background galaxy is lensed by another galaxy or cluster of galaxies in the foreground.

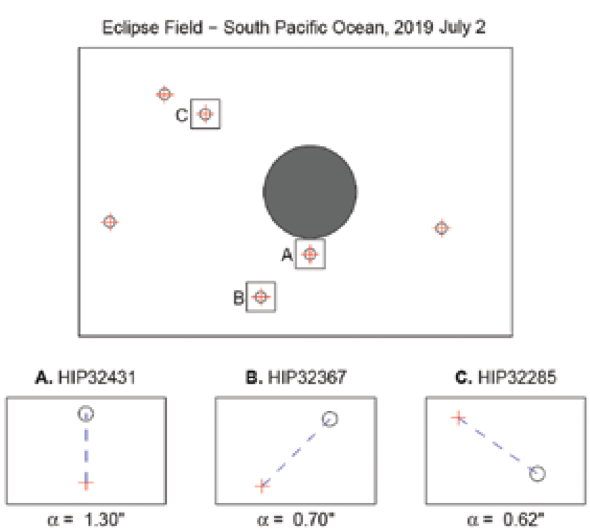

Figure 4 — Configuration of stars during the 2019 eclipse as seen from the Pacific Ocean. Note the large deflection of star "A".

Zwicky showed that when this is the case, the huge mass of an entire galaxy should provide a large enough gravitational field to significantly bend light in a way that might one day be observed. The effect was verified in the quasar pair *Q*0957+561A/B. These quasars are in fact not unique objects, but twin images of a single background quasar lensed by a foreground galaxy (Walsh, Carswell, and Weymann 1979). Since this discovery, hundreds of galaxy-scale gravitational-lens systems have been discovered. Today the lensing phenomena are seen from galaxy scale to systems lensed by entire clusters of galaxies (Kneib *et al.* 1996). Gravitational lensing provides a unique tool to directly measure the distribution of dark matter in galaxies (Dupke *et al.* 2007), the rate of expansion of the Universe (Refsdal 1964), the relationship between the masses of galaxies and their central black holes (Bandara, Crampton, and Simard 2009), and even allow the detection of extrasolar planets (Bouchy *et. al.* 2004).

Strong gravitational lensing, in which multiple arcs of background sources are produced, makes use of lensing masses as *natural telescopes* (Brewer and Lewis 2005). The lensing effect provides magnification in rough analogy with an optical lens, albeit one with a great deal of distortion, and reveals tiny details in the source objects that otherwise would not be resolvable with conventional telescopes. Modelling these systems allows astronomers to study both distant sources and the mass density of lenses simultaneously (Warren and Dye 2003). A number of schemes exist to perform this type of modelling (Koopmans (2005), Suyu *et al.* (2006)), and two of the authors have recently applied advanced global-optimization schemes to this kind of modelling (Rogers and Fiege 2011).

4. Results and Discussion

Armed with our *MATLAB* code and planetarium software, we investigated the first attempt to measure the gravitational lens effect by Eddington during the 1919 eclipse, shown in Figure 1. It is fortunate that the first such measurement was carried out in 1919, as the largest stellar deflection seen was $\alpha = 1.02''$, whereas successive attempts would not be as ideal. Our code was also used to simulate the lensing of starlight during a number of other eclipses, including the eclipse of 1979, which saw totality over Winnipeg, Manitoba (see Figure 2), and the upcoming eclipse of 2012, which will be visible from Cairns, Australia (figure 3). Note that the maximum deflection angles for these eclipses are $\alpha = 0.60''$ and $\alpha = 0.72''$ respectively, significantly less than the fortuitous 1919 eclipse. We have also calculated maximum deflection angles for all solar eclipses for the next 10 years, and found that a large stellar deflection should be seen during the eclipse of 2019 July 2, which will occur over the Pacific Ocean. Our calculation shows that the nearest star to the Sun during this eclipse has magnitude 6.5, and should show a displacement of $\alpha = 1.30''$, a larger deflection than was seen during the 1919 eclipse. Since this occurs 100 years after Eddington's initial expedition, there may be

Eclipse	Star	Right Ascension	Declination	Magnitude	Deflection α (″)
1919	HIP20842	4h 28.004 m	21° 37.254′	5.71	1.02 ± 0.05
	κ 2 Tauri	4h 25.406m	22° 12.061′	5.25	0.74 ± 0.04
	κ Tauri	4h 25.359m	22° 17.092′	4.18	0.62 ± 0.03
1979	HIP111761	22h 38.367m	− 7° 53.854′	6.21	0.60 ± 0.03
	HIP111577	22h 36.283m	− 7° 39.865′	7.00	0.45 ± 0.02
	HIP111414	22h 34.344m	− 9° 18.310′	8.46	0.39 ± 0.02
2012	HIP74728	15h 16.328m	− 18° 37.749′	8.15	0.72 ± 0.04
	TYC6174-106901	15h 19.450m	− 18° 17.308′	7.59	0.34 ± 0.02
	HIP74593	15h 14.467m	− 18° 25.717′	6.75	0.26 ± 0.01
2019	HIP32431	6h 46.173m	23° 22.288′	6.50	1.30 ± 0.07
	HIP32367	6h 45.389m	23° 38.774′	7.15	0.70 ± 0.04
	HIP32285	6h 44.411m	22° 34.744′	8.03	0.62 ± 0.03

Table 1 — Stellar positions are found directly from Starry Night Pro+ v6.0, which has a stated accuracy of 0.5". Using this value and the angular size of the solar radius, we have calculated errors for the deflection angles obtained from Equation 5. Deflection angles are calculated at the location and time of greatest eclipse as stated on the NASA Eclipse Web site.

some interest in performing a similar observation. For optical-deflection measurements, the July 2019 eclipse will provide an ideal situation, provided that this star is not obscured by the Sun's corona. This simulation is shown in Figure 4. Our eclipse results are summarized in Table 1.

5. Conclusions

Since Eddington observed the eclipse of 1919, verifying Einstein's prediction of the deflection angle at the limb of the Sun, gravitational lensing has grown as a valuable tool for the astronomical community to study a variety of wide-ranging phenomena. Measurements of the Sun's deflection angle made in visible light and later by radio interferometry have shown that GR correctly predicts the behaviour of light rays and verifies that the lensing effect is achromatic, acting on all electromagnetic radiation regardless of frequency. These observations have allowed astronomers to verify Einstein's theory to high precision. Using *MATLAB*, we have calculated the lensed positions of the background stars near the limb of the Sun for several solar eclipses, including Eddington's original observations of the 1919 eclipse at Principe, Africa. Our simulations show how tiny the deflections of starlight truly were, and highlight the practical difficulties of making these observations. Eddington's measurements were a *tour de force* of observational astronomy, resulting in the verification of the most profound theory of the cosmos yet developed. Furthermore, our eclipse simulations show that the eclipse of 2019, marking the centennial of Eddington's original expedition, will provide an excellent configuration of background stars to reproduce Eddington's results. ✶

References

Almassi, B. (2009). *Studies in Hist.and Phil. of Mod. Phys.*, *40*, 57

Bandara, K., Crampton, D., & Simard, L. (2009). *ApJ, 704,* 2, 1135

Bouchy, F., Pont, F., Santos, N.C., Melo, C., Mayor, M., Queloz, S., & Udry, S. (2004). *A&A, 421*, L13

Brewer, B.J. & Lewis. G.F. (2005). *PASA, 22*, 128

Dupke, R.A., Mirabal, N., Bregman, J.N., & Evrard, A.E. (2007). *ApJ, 688*, 2, 781

Dyson, F.W., Eddington, A.S., & Davidson, C. (1919). *Phil. Trans. Roy. Soc. A, 220*, 291

Einstein, A. (1905). *Ann. der. Phys.*, *17*, 821

Einstein, A. (1915). *Konig. Preuss. Akademie der Wiss., 844*

Einstein, A. (1936). *Science, 84* (2188),506

Fomalont, E.B. & Sramek, R.A. (1975). *ApJ, 199*, 1, 749

Harvey, G.M. (1979) *The Observatory, 99*, 195

Kennefick, D. (2007). eprint arXiv:0709.0685

Koopmans, L.V.E. (2005). *MNRAS, 363*, 1136

Kneib, J.P., Ellis, R.S., Smail, I., Couch, W.J., & Sharples, R.M. (1996). *ApJ, 471*, 643

Refsdal, S. (1964). *MNRAS, 128*, 307

Robertson, D.S., Carter, W.E., & Dillinger, W.H. (1991). *Nature, 349*, 768

Rogers, A. & Fiege, J.D. (2011). *ApJ, 727*, 2, 80

Schmidt, M. (1963). *Nature, 197*, 1040

Soldner, J.G.v. (1804). On the Deflection of a light ray from its rectilinear motion, by the attraction of the body at which it passes by, *Berliner Astronomisches Jahrbuch,* 161

Suyu, S.H., Marshall, P.J., Hobson, M.P., & Blandford, R.D. (2006). *MNRAS, 371*, 983

Treuhaft, R.N. & Lowe, S.T. (1991). *AJ, 102*, 5, 1879

Warren, S.J. & Dye, S. (2003). *ApJ, 590*, 2, 673

Walsh, D., Carswell R.F., & Weymann R.J. (1979). *Nature, 279*, 381

Will, C. M. (1993) *Was Einstein Right?: Putting General Relativity to the Test,* (New York, Basic-Books)

Zwicky, F. (1937). *Phys. Rev., 51*, 290

Unique Space Club For Young School Kids

by Ray Bielecki
(ray.bielecki@cbc.ca)

The "Astronuts Kids' Space Club" started out a year ago as "Brett's spaceship under the stairs." My 8-year-old son Brett and I spent countless hours building Spaceship Mercury One in a space under the recreation-room stairs. We spent our time looking at star charts, dreaming our way through the Cosmos, and building and rebuilding the many cardboard boxes that had become our space-ship home. It was all held together by glue sticks, duct tape, and dozens of strings of twinkle lights.

Space Ship Mercury One (SSM-1) soon became a gathering place for Brett's friends seeking adventures in space. The space explorers left the safety of the spaceship carrying black-light space guns, stopping only to refresh with *space ice cream!* Last spring Brett and I created the Astronuts Kids' Space Club in order to give all these early elementary school kids the chance to learn about space, science, and astronomy. NASA, the Canadian Space Agency, and a number of Canadian and U.S. astronauts have encouraged us to learn and grow!

The *crew* of 12, boys and girls aged 8 to 9, meet monthly at our Newmarket home (better known as Spaceship Mercury Two (SSM-2). The *missions* are two hours long and include science experiments, engaging presenters such as Alan Nursall (Daily Planet/Discovery Channel), Bob McDonald (host of CBC *Quirks and Quarks*), amazing *Skype* guests such as the father and son of the "Brooklyn space program," rocket launches, and *spin the magic space wheel*. This is a game where the astronuts get to spin a big wheel for space prizes if they answer a science skill-testing question.

Space Ship Mercury One was scuttled last month to make room for the assembly of the larger Space Ship Mercury Two. If you visit our Web site, www.astronutskidsspaceclub.com, you can see all about our missions and other activities.

One goal of the club is to learn about astronomy. "Mission #4" had a theme of astronomy and was led by François ven Heerden of the RASC Toronto Centre. He is an amazing and engaging presenter. The *astronuts* really enjoyed his solar-telescope demonstration and were *wowed* by the solar flares we could see through the instrument. François has been a growing part of the kids learning about astronomy. Special thanks go to RASC members Ron Macnaughton, Ralph Chou, and Julie Tome for setting this up.

Both Julie Tome (RASC) and Paul Delaney (astronomy professor at York University) had a terrific interactive craft session with the astronuts in Mission #5. It was all about astronomy and *create your own planet*.

Figure 1 — The author and his son preparing for a solar space mission.

We just finished Mission #6, where we were hosted by the Ontario Science Centre. In this mission, we toured the Space exhibit with a pair of *white-lab-coat* OSC space and astronomy scientists, Jesse and Rob. They thoroughly entertained and educated the astronuts on all things that twinkle and shoot across the night sky! They also treated us to a private planetarium show.

Brett and I were recently invited to the Canadian Space Summit, hosted by the Canadian Space Society. We were taken on an amazing tour of the Canadian Space Agency's David Florida Laboratory to view Canada's contribution to the *James Webb Space Telescope*, a fine-guidance system!

We really love what we have created and the smiles on the faces of these future astronauts, scientists, and astronomers.

Please go to our Web site to learn more about us at www.astronutskidsspaceclub.com ✶

Building Sustainable Communities Conference, 2010 November 15–18

by Robert Dick, RASC Light-Pollution Abatement Program (rdick@carleton.ca)

Introduction

The need to reduce light pollution must be promoted beyond the RASC to authorities who can implement lighting policies based on principles of light-pollution abatement (LPA). An efficient technique to reach this goal is to speak at meetings of planners and policy makers. LPA is not on the agenda of most cities, so it must be introduced by riding on the back of more popular and politically energized subjects such as sustainability. The RASC funded our attendance at the 2010 Building Sustainable Cities Conference in Kelowna, B.C. This article summarizes the rationale for our attendance and the items covered in our presentation.

The Conference

In mid November, on behalf of the RASC, we attended a conference in Kelowna, B.C., on sustainable communities. As with most professional conferences, it was held in the comfortable surroundings of the large Delta Hotel (Figure 1). This was not a conference you would expect an astronomer to attend. However as the Chair of the RASC Light-Pollution Abatement Committee, this conference was a very good place to be.

Most members of the RASC bemoan the growing blight of light pollution, driving 10 or 50 km farther from their home than they did in the previous decade in search of dark skies. We are sure most readers would like to speak to the people who approve the planning and installation of lighting – perhaps to make them aware of the impact that lights are having on astronomy and, more importantly, the environment. Although a few concerned individuals can politely make officials aware of light pollution, if all 4000 members of the RASC applied pressure, it might be such a nuisance that it may become counter-productive. More focussed and crafted presentation seems to be most effective. The role of the RASC membership-at-large can be used to increase awareness of light pollution through displays, public presentations, and public star parties.

Figure 1 — Grand Delta Hotel and Convention Centre in Kelowna, B.C.

Few citizens look up into the night sky and decide to make light pollution a burning social issue. But light pollution affects more than just astronomy. There are effects of outdoor artificial light at night (ALAN) on our physical and mental health. I don't mean effects to our mental health caused as we bear the frustration and sense of helplessness when confronted by increasing urban sky glow. It has a more basic impact, on our memory and cognitive functions. These topics are very different from astronomy and well beyond the knowledge set of most astronomers. I would suggest these topics are more complex, because they cover several fields of research: biology, biochemistry, physiology, and psychiatry.

It is not fair to require all LP activists to become aware of all these fields because there would be no time left for observing. (Believe me, I know.) My personal studies into these subjects over the last eight years has given me a superficial understanding of the material as it pertains to ALAN and has led to discovering the science of scotobiology – the biology of darkness. In response, we have created the Canadian Scotobiology Advisory Group.

Light pollution is no longer just an astronomer's problem. Ample research in ecology and medicine support the hypothesis that ALAN causes physical and mental maladies that are taxing our public-health system and changing the environment. The International Agency for Research on Cancer (IARC) of the World Health Organization and the American Medical Association have identified light at night as a health risk.

What better place to promote reductions in light pollution than at a conference with a theme of the sustainability of human activity? (Dare I say the human civilization?) The conference in Kelowna attracted over 400 municipal planners, councillors, and facility managers from across British Columbia and the Prairie provinces. These were the people who are in the position to change existing urban lighting practices.

There were six concurrent sessions filling rooms that could hold from several hundred people to a few dozen participants (Figure 2). I was scheduled in an intermediate-size room along with the Suzuki Foundation and topics on bio-waste, policy of Green Jobs, use of green energy, and building sustainable economies with carbon-offset strategies. Other major topics covered in the sessions were the reduction in energy use, efficient use of surface and ground water, urban gardens, and district heating. The delegates to whom I spoke during the sessions and *off-line* were not aware of the adverse health effects of artificial outdoor lighting and were very interested in hearing more about it. I obliged with follow-up emails.

continued on p. 70

Pen & Pixel

Figure 1— Sanjeev Sivarulrasa of the Ottawa Centre captured 44×30 arcminutes of Pegasus near the spiral galaxy NGC 7331. Above the galaxy are four fainter – and much more distant – background galaxies sometimes referred to as "the fleas" or "the Deer Lick Group." In the lower left corner of the image is Stephan's Quintet (Hickson 92). Sanjeev used a f/7.3 TEC140 refractor with a QSI 583ws CCD camera and Astrodon GenII LRGB filters. Exposure was 100:40:20:40 minutes in LRGB, (3 hours 20 minutes in all) from the parking lot of the Ottawa Centre's Fred Lossing Observatory.

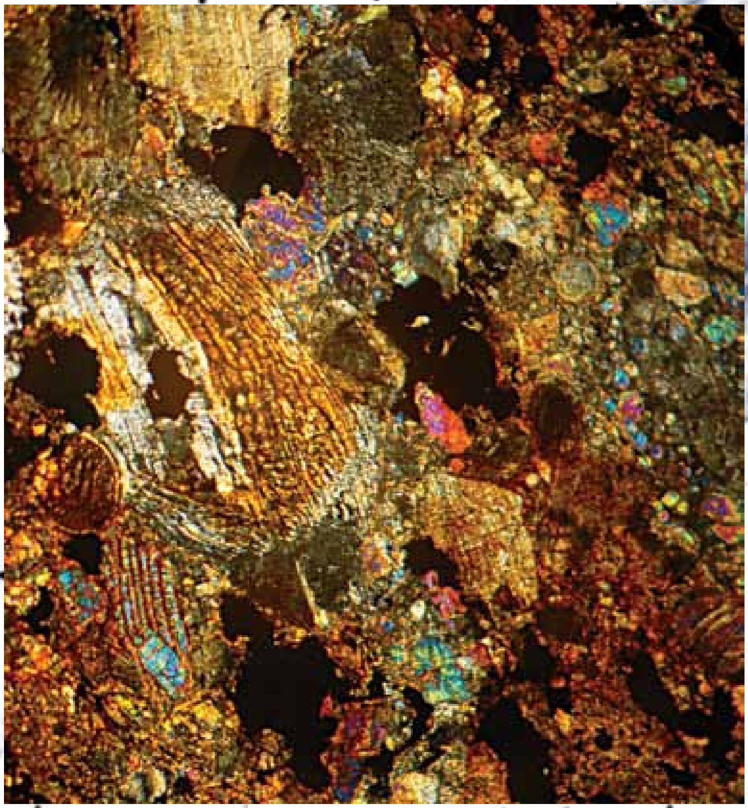

Figure 2 — Winnipeg Centre's Ralph Croning collects meteorites. Seen here is a thin section of the Gold Basin meteorite, photographed through a microscope in cross-polarized light. This method of viewing shows interference colours that can be used to identify mineral content. The black areas are metal (Fe-Ni). The circular inclusions are pristine chondrules, while the others have deformed due to impact shock and/or melting and re-crystallization. Ralph sandwiched the thin section between two photographic polarizing filters and rotated them until he had the desired colours. Magnification is about 35×.

Figure 3 — James Black used his super-fast C14 with its f/2 Hyperstar configuration to capture "The Divide" in this 77-minute (11 × 7 min) image of the region between the North America Nebula and the Pelican Nebula. James used a Starlight Express SX-M25C one-shot-colour camera from a site at Pitt Meadows, east of Vancouver on June 10 last year.

Figure 4 — Stephen J. McIntyre turned to an old favourite and then turned a little to the side to image the globular cluster M13 and its close-by 11th-magnitude galaxy partner NGC 6207. Stephen used an exposure of 15 x 4 minutes at ISO 400 on a modified Canon XS/1000d attached to an Impression 173-mm f/5.7 Newtonian reflector.

Figure 2 — Main meeting room for Sustainability Conference

The only reference in our talk to astronomy was in a slide used as *eye-candy* (Figure 3). The talk focussed on the impacts of ALAN on our circadian rhythm, vision, crime, and municipal *bottom lines*, and we presented a few techniques for lighting and navigation that have been applied in Canadian Dark-Sky Preserves.

We acknowledged that our society has benefitted from light at night. After having visited a few very large cities in North America, many citizens seem to rate the benefits of our 24/7 lifestyle higher than the consequences, and they are not inclined to change. We raised the issue that white-light luminaires may keep us alert at night, but at the cost of our long-term health. As with most technical developments, technology has changed the environment to which we have evolved – altering the ecological balance and undermining our health.

The weeks after the conference involved continuing conversations initiated during the meeting. There were numerous requests for more information. We can appreciate that ALAN and its impact on our health is a new concept that requires more in-depth information than can be presented in a 30-minute talk. Conversations and contacts at the conference have led to the submission of four articles in national and provincial trade magazines and newsletters. The conference was only the beginning of an effort that will last for a few more months in the wake of the meeting.

Coincidentally, the Okanagan Centre of the RASC was having a meeting in Kelowna during our visit. After their business meeting, we gave a presentation about the effect of nighttime use of white LEDs on our vision and our health.

With our attendance at this conference, we were able to put lighting on the agenda of many municipalities, both as a topic for sustainability and as an option for reduced energy use. We cannot expect immediate results, but perhaps a few communities will be a decade ahead of the inevitable progression towards darker skies and a healthier environment.

Acknowledgements:

We would like to thank Alan Whitman (Okanagan Centre) for proposing, and the RASC National Council for approving, sufficient funds for our attendance at this conference. Without this attendance, there would have been fewer opportunities to raise light pollution as an environmental and health issue.

The draft text of our presentation is available from the author (1 MB pdf) ✶

Figure 3 — Simulated view of sky over Bruce Peninsula Dark-Sky Preserve

Pen Henge

by Dave Gamble, Okanagan Centre
(trailspublishing@telus.net)

The mystique attached to standing-stone structures such as Stonehenge embraces much more than just their origin and antiquity. Not many people could escape experiencing a chill up the spine if they witnessed the Sun dramatically rising or setting in direct alignment with the enigmatic stones.

As part of its International Year of Astronomy activity in 2009, members of the Okanagan Astronomical Society of Penticton, B.C. (which last year became the Penticton meeting group of the RASC Okanagan Centre, joining Kelowna and Vernon) hit upon the idea of constructing a standing-stone array of their own. The result has now been completed and *Pen Henge* was officially dedicated at a 2010 December 21 winter solstice event.

The genesis of the project occurred when participating OAS members, led by DRAO scientist Chris Purton, scheduled an IYA summer-solstice event on 2009 June 21 to watch the Sun set at its most northerly point. The location chosen for the event was Munson Mountain, a volcanic hill overlooking Okanagan Lake near Penticton. Visitors may recall seeing a large *Penticton* sign etched into a hill across the lake from the highway. The solstice event took place on the hilltop, just above the sign.

During the observance, Chris and the committee hammered spikes decorated with strips of fluorescent tape into the ground to mark the direction of the observed summer-solstice sunset. The markers were installed in consultation with Penticton City Parks, following correct procedures for ground penetration, with the spikes set right into the ground for safety reasons.

In the fall of 2009, Chris approached the Penticton Parks and Recreation Advisory Committee with a proposal for erecting permanent sunset markers on site. The proposal was received enthusiastically despite concerns about safety, as the project would draw people to the top of the hill, an unmaintained part of the Park with dangerously steep sides. Penticton Council gave the go-ahead under the condition that access paths be improved, and that a fence be installed along the steepest edge. The project landed in the lap of Penticton Parks Supervisor Jeff Lynka to oversee, and he provided tremendous support and a lot of help throughout.

The initial proposal was that the project would be undertaken by the Okanagan Astronomical Society, using fairly small field stones anchored to the ground with lengths of reinforcement bar (rebar) cemented into holes in their bottoms, at no cost to the City. It turned out, however, that funds were required, and these were allocated by the City, partly for the upgrades to the mountaintop and partly for machinery to help install the larger stones on which virtually everyone insisted.

Later in 2009, and into the following year, markers were placed for the equinoxes and for the winter solstice. By the time of summer solstice in 2010, the work had to be done again, as the spike from the previous year had disappeared. Chris remarked that he thought it was something of a miracle that the spikes lasted in place as long as they did, and this thinking contributed to an approach for permanently securing the future stone markers in place.

In the summer of 2010, the members scoured the countryside for suitable stones. The heel stone and the equinox stone were both found in a rock cut on the old Kettle Valley Railway right-of-way on the west side of Skaha Lake, and the two solstice stones were secured from a rockslide some distance out, along the Ashnola Road in the Similkameen Valley.

The stones were prepared by Chris, who drilled three holes in the bottom of each and fabricated carefully aligned jigs to precisely locate the holes that were to be drilled into the bedrock at the four sites. To ensure the stones were permanently secured, three lengths of rebar for each stone were cemented into the holes in bedrock, and these were in turn cemented into the holes on the bottom of the marker stones.

Figure 1 — A backhoe, assisted by (l-r) Jordy Bouillet, Jim Shaver, and Chris Purton, was used to align three holes drilled into the bottom of the ~225-kg heel stone with lengths of rebar that were cemented into the bedrock to firmly secure the markers.

Figure 2 — Over 80 people gathered on top of Munson Mountain, overlooking Penticton, to participate in the official dedication of the Pen Henge stone array. Near the podium at the left is the heel stone with the summer solstice stone in the foreground, the equinox stone to the right, and the winter solstice stone behind onlookers.

The heel stone was the first one to be installed, in late September. In that location, the glacial till was fairly deep, so the rebar was cemented into a large concrete block that was provided by the city and buried below the marker. The three seasonal marker stones were installed during two work parties in late October.

The Pen Henge Concept

In its finished form, Pen Henge consists of four stones that mark the direction to the sunset points for the four seasons. The *heel stone* on the eastern side of the hill top lines up with the stone to the southwest to show exactly where the Sun drops behind the hills at the time of winter solstice; the northwestern stone is for the northernmost sunset at summer solstice, and the middle stone marks the vernal and autumnal equinoxes on the equator.

A brass plaque with a brief explanation of the array will be permanently attached to the top of the heel stone.

Chris noted that, though the stones weighed in at approximately 225 kg each, they were kept reasonably small by design with the idea that they would blend in with the natural look of the place. A casual visitor would not know they had any particular significance unless he or she noticed the plaque.

"For most of the year the structure simply illustrates the enormous range along the western horizon where the Sun sets," Chris noted. "Most people subconsciously know of this, but they are quite fascinated to see the idea laid out so graphically. Virtually everybody to whom I've mentioned the project thinks it is a great idea, and most often they think of Stonehenge right away."

Chris observed, "The time of winter solstice is, of course, special for this project. On that day, anyone on the mountain at sunset would see the Sun slowly sink to the horizon. As it slid out of sight, an observer located behind the heel stone would see the Sun lined up right over the winter solstice stone. At the same time, the shadow of the winter solstice stone would be getting longer, and slowly swinging around to point directly at the heel stone as the Sun sets. Anyone standing on the winter solstice stone, or in front of it, would see their own shadow do the same thing. This all depends, of course, on the sky being clear right down to the horizon." The scene would be similar for the summer solstice.

From an astronomical point of view, Chris noted an interesting point: while the direction to the sunset point is the same for both equinoxes, the times are different. He explains: "In fact, the only part of the whole array of times that is easily calculated is the difference between sunset times for the two equinoxes, which requires only the equation of time. In principle all the times are calculable, but would need a survey of the profile of the hills to do it."

At the Pen Henge location, the actual times when the Sun sets on the horizon for the four events are: winter solstice 3:27 p.m. PST; vernal equinox 6:35 p.m. PDT; summer solstice 8:58 p.m. PDT; and autumnal equinox 6:20 p.m. PDT.

While clear skies failed to materialize for the official dedication during the winter solstice on December 21, it didn't prevent over 80 people from attending the event. The hilltop program was led by Chris Purton, who explained how the project came to be and how it worked. To mark the actual instant of solstice, Chris rang a cow bell at 3:38 p.m. PST, and RASC Okanagan Centre Penticton meeting group Vice-

President Ryan Ransom dedicated the bronze plaque that will be permanently mounted on the heel stone.

The gathering then retired to the Okanagan School of the Arts Shatford Centre in Penticton for refreshments, displays, and a short talk that included discussions about ancient solstice ceremonies: those at Stonehenge, among the local Syilx First Nations, the Roman's Sol Invictus, Brumalia traditions, as well as Christmas.

Interestingly, the Okanagan School of the Arts' emerging Shatford Centre in Penticton already included plans to highlight the beginning of each season in some special way, which fits in very well with the Pen Henge project.

Organizers are now hoping for clear spring skies when they gather to mark the vernal equinox in March. ✶

Dave Gamble was elected president of the RASC Okanagan Centre last fall. He has had a lifetime interest in astronomy, and enjoys observing and imaging from his observatory in Summerland, B.C., as well as at the club's Okanagan Observatory, which houses the 25-inch telescope he helped to build.

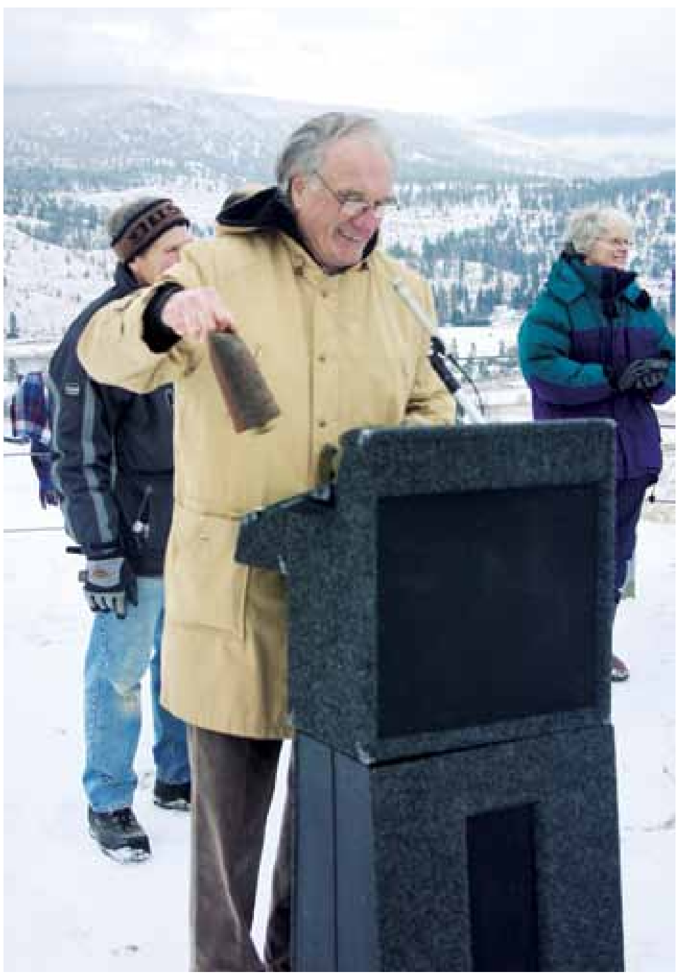

Figure 3 — At 3:38 p.m. PST on December 21, Chris Purton rang a cow bell to officially mark the moment of the winter solstice, and to inaugurate the new Pen Henge stone array.

WWW

RASC Internet Resources

www. rasc.ca

Visit the RASC Web site

www. rasc.ca/discussion

Email Discussion Groups

www. rasc.ca/contact

Contact the National Office

www. rasc.ca/rascnews

RASC eNews

Cosmic Contemplations

The Digital Schmidt Camera

by Jim Chung, Toronto Centre
(jim_chung@sunshine.net)

Like most guys, I'm an inveterate tinkerer. I think my Dad may have passed it on to me as I watched him fix appliances and lab equipment. Typically all that was required was a thorough cleaning and lubrication, but that was back in the days before designed obsolescence, the days before plastic gears and rubber belts, and the days before you needed a black box to diagnose your black-box problems.

Recent winters in the Toronto region have been persistently cloudy and have severely reduced the number of clear nights available for imaging. This year I've occupied myself with a number of ATM (amateur telescope making) projects, in particular the digital conversion of a 1970s-era 8-inch Celestron Schmidt camera.

At the turn of the last century, most of the large observatory telescopes were Newtonian reflectors. Their combination of small field of view (FOV), slow optics, and off-axis coma were serious obstacles to film photography. Several nights and numerous exposures would be needed to document an extended nebula, and this limitation hindered deep-sky photography for two decades. It would seem that a short-focal-length primary mirror would be the obvious solution; however it is technically very difficult to precisely grind a fast, large-diameter paraboloid. Coma also increases proportionally with diameter and inversely with the square of the focal ratio of the mirror.

In 1931, an obscure Estonian optician named Bernhard Schmidt proposed a design that offered a flat, distortion-free, large FOV and extremely fast optics. Unfortunately, Schmidt died in 1936 and, like van Gogh, never experienced his due recognition. At least his family can celebrate the thousands of scopes that bear his name today. In 1949, the famous 48-inch f/2.5 Schmidt camera was constructed at Palomar and began its revolutionary seven-year sky survey of the Northern Hemisphere. This was arguably the most important scientific achievement responsible for our current understanding of the cosmos. In contrast, it would have taken the 200-inch Hale reflector 10,000 years to finish the same survey!

Figure 1 — Comet Hale-Bopp. Image by Dan Schechter.

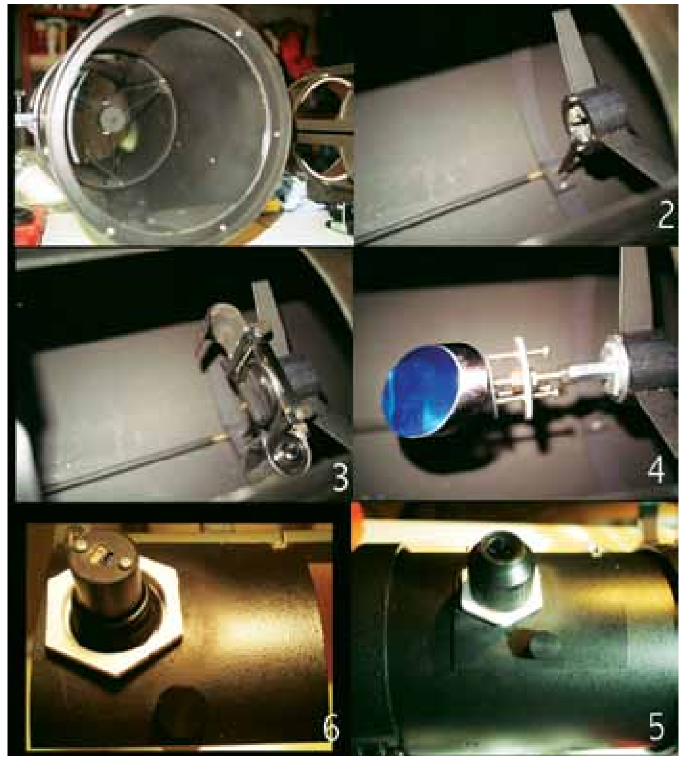

Figure 2 — Modifications to the Celestron Schmidt.

One of the best film images that I have ever seen was sent to me by Dr. Dan Schechter of California. He took this image (Figure 1) of Comet Hale-Bopp with an 8-minute exposure using Fuji 100 35-mm print film and his Celestron 8-inch Schmidt camera. Talk about perfect stars from corner to corner!

Digital-imaging technology was preordained to be integrated with the Schmidt camera. The Catalina Sky Survey is an array of Schmidt cameras with CCD sensors in place of film, designed to track and catalogue near-Earth objects. Even comet hunter David Levy had his Meade 12-inch Schmidt camera converted to digital with a highly modified SBIG STL11000 CCD – a change that now allows him to take scores of 3×2-degree images each night, capturing stars down to 18th magnitude. Contrast this to the old days when he used hypersensitized Kodak B&W film and could take at most ten exposures per night – and still had to develop them in the morning after staying up the entire night.

I was motivated to convert my Schmidt camera for astro outreach applications. The incredibly fast f/1.5 optics would allow almost real-time narrowband imaging, permitting the public to see deep-space objects in high-contrast video from within the city. To try to purchase a 300-mm-focal-length camera lens at f/1.5 would be either impossible or cost in the tens of thousands of dollars.

The Celestron Schmidt consists of an 8-inch spherical primary mirror and a zero-power aspheric corrector plate (Figure 2, 1) to correct spherical aberration. A three-vane spider (Figure 2, 2) suspends a 35-mm film carrier (Figure 2, 3) on special rods made of zero-expansion Invar with the focus preset at the factory. The focal plane of the camera is curved and the carrier deforms the film negative to follow this curve precisely. Similarly, each glass plate of the Palomar Sky Survey had to be deformed with a special jig before being placed in the camera. I didn't want to alter the focus position of the spider in case I want someday to experiment with film. Placing a CCD/camera inside the tube increases the size of the central obstruction and introduces the complexity of liquid cooling – you don't want a fan blowing hot exhaust air in there! So I rigged up a secondary mirror (Figure 2, 4) that snaps onto the spider's magnetic coupler and allows an eyepiece (Figure 2, 5) or CCD to be placed outside the loading port. The external hole is lined with PVC pipe fittings that function like a helical focuser.

The only CCD I had that was small enough to fit inside the 2-inch barrel was my Starlight Express Lodestar guide camera (Figure 2, 6).

Using a 7-nm-bandwidth Hα filter, I was able to image M42 and the Running Man Nebula quite thoroughly in 1 minute. The Horsehead Nebula was clearly visible after a 2-minute exposure. Both images show stars in the periphery starting to defocus due to the nonconformity of the CCD's flat imaging plane. A field-flattening plano-convex lens placed in close proximity to the CCD can alleviate this problem.

I am never one to leave well enough alone and, at the time of writing, I was still in the midst of creating a remote APS-sized CCD head by removing the sensor board from an old Canon 10D DSLR (Figure 4) and reconnecting it with a longer, flat, flexible cable to the camera motherboard. Isolating the sensor will allow it to be placed just inside the film loading port, in position to come to focus and allow the correct placement of the plano-convex lens (Figure 5). The large chip will be better able to showcase the wide FOV than the $^1/_2$-inch Lodestar chip. I'm confident that it will be a valuable outreach tool, and for that cause, you will find me frequenting the grounds of the David Dunlap Observatory this summer. ✶

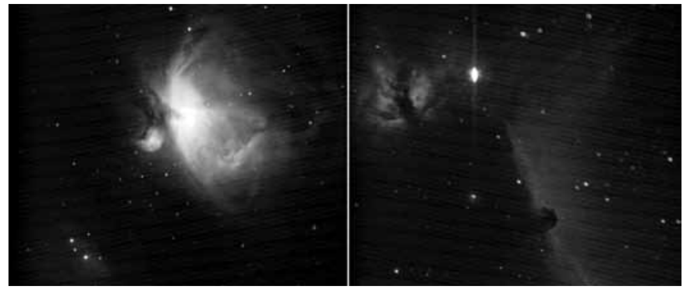

Figure 3 — M42 and the Horsehead Nebula area taken with the Lodestar CCD through the modified Schmidt Camera

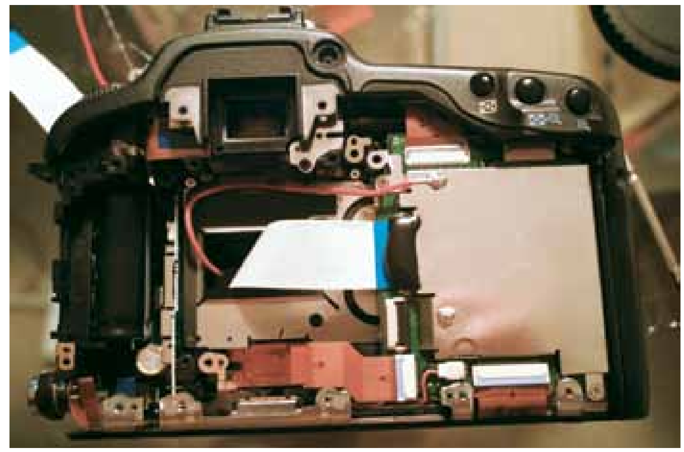

Figure 4 — The Canon 10D after modification.

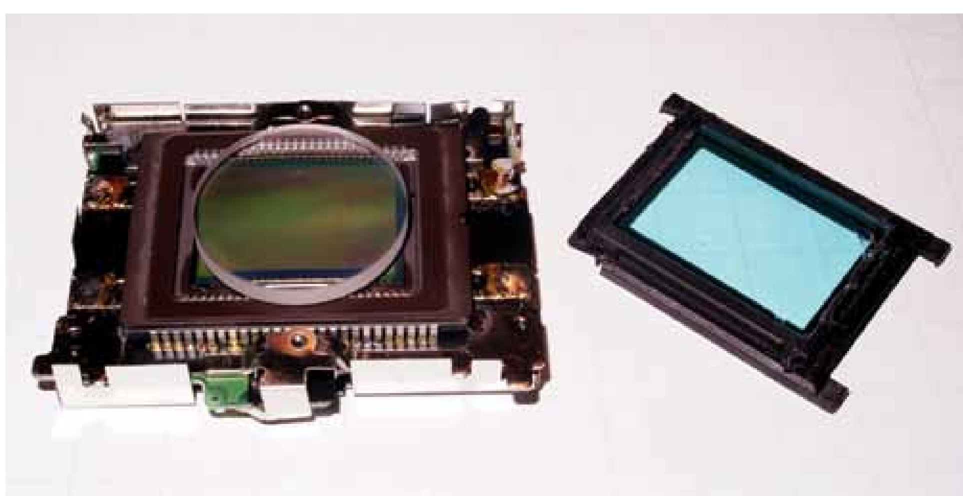

Figure 5 — The Canon 10D with field-flattening lens superimposed.

Jim Chung has degrees in biochemistry and dentistry and has developed a particular interest in astroimaging over the past four years. He is also an avid rider and restorer of vintage motorcycles, which conveniently parlayed into ATM projects, such as giving his Skywatcher collapsible Dobsonian a full Meade Autostar GOTO capability. His dream is to spend a month imaging in New Mexico away from the demands of work and family.

The Iris Nebula in Cepheus

by David Garner, Kitchener-Waterloo Centre
(jusloe1@wightman.ca)

Cepheus is always there in the northern sky and you don't have to look long or hard to find it. Some describe it as house-shaped; to others it is a pentagon with its five stars. The brightest star, alpha Cephei or Alderamin, can be found at the bottom-right corner, opposite zeta Cephei at the other bottom corner. Gamma Cephei is at the peak of the house and, due to Earth's precession, is expected to become our pole star in about 2000 years.

Very close to zeta Cephei, near the bottom-left corner, you might take time to observe delta Cephei. This is the prototype star for Cepheid variables. Cepheid variables with their pulsation periods are used as standard candles for galactic and extragalactic distance measurement. Delta Cephei ranges from magnitude 3.6 to 4.3 over a period of 5.36 days. If you want to try observing variable stars, this is the one to start with.

Other objects in the Cepheus area include a large emission nebula known as IC 1396, the open cluster M52, the Bubble Nebula, the Cocoon Nebula, and the Iris Nebula. The Iris Nebula (Figure 1) is a bright reflection nebula surrounding the cluster of stars NGC 7023. It is located about 3.5 degrees southwest of beta Cephei, the top-right corner of the house.

NGC 7023 was observed in 1794 by William Herschel. The nebula surrounding this cluster is illuminated by the light from a young, hot B2V star, HD200775, located at its centre. The nebula has been shaped by the star-forming process, leading to the creation of a cavity in the parent dust and gas cloud. Blue light from the central star is reflected off the thick mounds of dust particles in the dense nebula, giving the object its unusual petal-like structure and its name, for its resemblance to an iris flower.

There are faint hints of red colour surrounding the central star that indicate some hydrogen-light emission at 656 nm is taking place. In addition, several researchers studying the dark regions surrounding the nebula are finding broad emissions ranging from 540 to 900 nm. This Extended Red Emission (ERE) is the result of photoluminescence of dusty hydrocarbon molecules exposed to ultraviolet (UV) photons. ERE caused by UV photons has been observed in many other environments, such as the diffuse interstellar medium, various reflection nebulae, and planetary nebulae. Astrophotographers might wish to consider these wavelengths as they practice their art.

The Iris Nebula can be found at RA $21^h\ 01^m\ 35.60^s$ and Dec +68° 10′ 10.0″ (Figure 2). With an apparent magnitude of 6.8, it is estimated to be 1300 ly distant and about 6 ly across. To get a close-up of the Iris Nebula there is a beautiful video on *YouTube*: www.youtube.com/watch?v=pQUJMdVKnoI&feature=player_embedded ✶

Figure 1 — The Iris Nebula, courtesy of Ron Brecher, K-W Centre. Image acquired using a QHY8 camera (Gain=0; Offset=125) with UV/IR filter and a 152-mm refractor at f/8 on an MI-250 mount. The mount was guided using PHD *software and the KwiqGuide system. The calibration was done in* Images Plus 3.0. *Alignment, stacking, and processing exclusively using* PixInsight.

Dave Garner teaches astronomy at Conestoga College in Kitchener, Ontario, and is a Past President of the K-W Centre of the RASC. He enjoys observing both deep-sky and Solar System objects and especially trying to understand their inner workings.

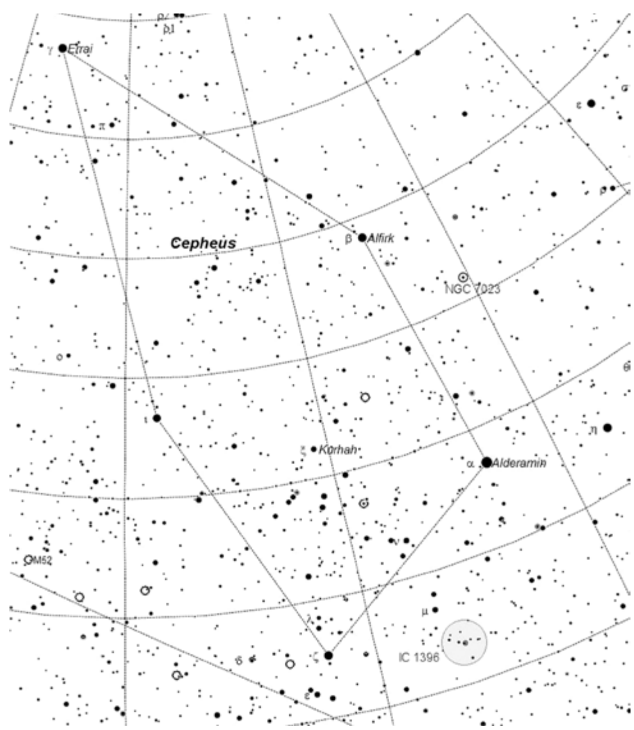

Figure 2 — A map of the constellation Cepheus.

A Moment With…

Dr. Brett Gladman

by Phil Mozel, Toronto and Mississauga Centres (dunnfore@gmail.com)

If you don't mind, pull out your copy of the *Observer's Handbook*; I'll wait … OK, now turn to the section dealing with the natural satellites of the planets and look down the *Discovery* column. Listed more than two dozen times are moons whose discovery involved Canadian scientists. One is Dr. J.J. Kavelaars; the other is Dr. Brett Gladman, the subject of this issue's column.

Back in high school, Dr. Gladman was turned on to astronomy when he learned of Dr. Werner Israel's work at the University of Alberta on black holes. Intriguing as he found these objects, Dr. Gladman realized he liked scientific problems where there was more abundant data and thus opted to study objects in the Solar System and to try to learn how the Solar System came to be. He now studies its formation, evolution, and dynamics. He might be thought of as a planetary palaeontologist: since the planets don't retain a lot of information about their origins, he hunts *fossils*, *i.e.* some of the Solar System's more primitive bodies that may contain information about its earliest days.

But, back to Dr. Gladman's satellites. Take a look at the properties of these objects. For one thing, they're tiny, the largest being just 32 kilometres across and the smallest a mere 2 kilometres. This makes for tough sledding, observationally speaking! And, look at those orbits! They all lie outside the plane of their planet's equator and outside the orbits of the largest satellites. Many of their orbits of these tiny moons are far out-of-round as well. These orbital properties, along with their generally small size and usually far-from-spherical shapes, qualify them as *irregulars*.

The discovery of irregulars really began to ramp up in the late '90s, when Dr. Gladman and his colleagues turned the then-new COSMIC camera of Mount Palomar's 5-m Hale Telescope to Uranus. COSMIC did double duty as both a spectrograph and direct-imaging camera optimized to photograph faint objects. At the time, its 10-arcminute field-of-view on a 5-metre telescope was huge (although it is now small by CCD-mosaic camera standards). The moons Caliban and Stephano, both dimmer than magnitude 22, were pulled from the background noise in 1997 and 1999, respectively.

In 2000, Dr. Gladman (then at the Observatoire de la Cote d'Azur in France) and his colleagues located three new irregulars of Saturn – the first new irregulars after Phoebe – using the European Southern Observatory's 2.2-m telescope in Chile. Later that year, they used the Canada-France-Hawaii Telescope (CFHT) to confirm the discovery and to locate nine more moons! After moving on to Jupiter in 2003, Dr. Gladman helped bag nine more irregulars. In 2003, again using the CFHT, plus the Cerro Tololo Inter-American Observatory's 4-m, the team found five Neptunian irregulars. This was something of a relief since, based on the discoveries around Jupiter, Saturn, and Uranus, it was expected that Neptune too would have a coterie of small moons. Now it did.

Dr. Gladman has referred to the rich haul of irregulars as the opening of Pandora's Box: a lot of questions about their origins have been raised. Were they captured? If so, where did they come from? Was their source the Kuiper belt? Or, did they form from planetesimals in orbit around the Sun near their planet and then were captured? If so, what can this tell us about the origin of the planet itself? Dr. Gladman cites the example of Phoebe: if it formed near Saturn, it is a uniquely preserved large object from the protosolar nebula. If it's from the Kuiper belt, it's a dime-a-dozen.

It does seem, however, that irregulars were almost certainly captured during the early stages of planet formation. This does not mean that what we see now is what existed in the past. Collisions have probably played a role in their characteristics. For example, based on colours and orbits, one can surmise that certain irregulars belong to groups or families that were at one time a single, captured object. A case in point is the 12 Saturnian irregulars that exhibit orbital clustering, implying derivation from just a few parents.

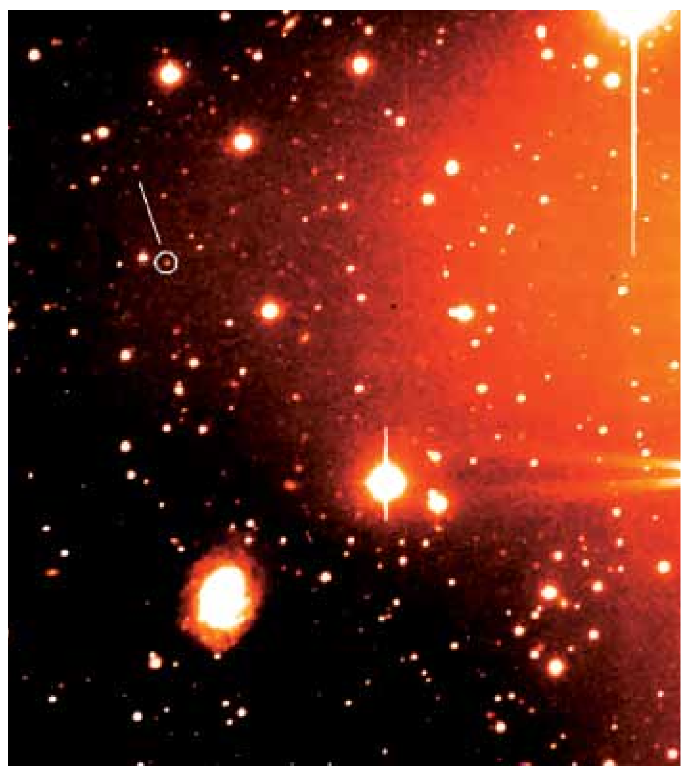

Figure 1 — The discovery image of Caliban (S1997 U1), captured by Brett Gladman, Phil Nicholson, Joseph Burns, and J.J. Kavelaars using the Hale 200-inch telescope on Mount Palomar. The moon is about 80 km in diameter.

In 1998, the first binary Kuiper belt object (other than Pluto) was discovered. Astronomers with an interest in Solar System dynamics, such as Dr. Gladman, find these binary objects of considerable interest since they can take only so much gravitational bullying before being torn from each other. This puts constraints on Solar System formation processes. An example is 2001 QW322, whose components are separated by up to a rather large 135,000 kilometres (a third the Earth-Moon distance). Prone to orbital disruption, it has probably been a pair for *only* about a billion years.

In 2004, the high-inclination trans-Neptunian object 2004 XR190 (nicknamed *Buffy*) was discovered during the course of the Canada-France Ecliptic Plane Survey. In 2008, the first Kuiper belt object with a fully retrograde orbit was detected: 2008 KV42 *(Drac)* has an orbital inclination of 104 degrees, coming inside the orbit of Uranus and swinging out as far as 70 astronomical units.

What are we to think of all these highly inclined, distant, sometimes double bodies? Dr. Gladman says that something weird is going on, and, while there are no good theories to explain how the orbits of many of these objects evolved to their present form, he does have some ideas. In the Oort cloud, there is a vast reservoir of comets that can drop in on us from any direction, while comets with prograde, low-inclination orbits come from the Kuiper belt. He believes that the weird objects come from a large, as-yet-undetected third reservoir (with highly inclined orbits) between the Oort cloud and Kuiper belt. These leftovers of the Solar System's birth are the few survivors of a much greater population scattered by the gravitational influences of the larger planets. Hopefully, these survivors will be able to tell us much about that process.

The planets responsible for scattering these minor worlds may not only be the ones we see today. I asked about the possibility of another major planet in the Solar System's outer reaches, one that had helped gravitationally to produce its current structure. Dr. Gladman feels that it makes no sense to just have had (4 billion years ago) some dwarf planets plus the current gas giants with their ten-Earth-mass rocky cores. There should be some intermediate objects, too. There may not be many of these planets left – they "stir the pot" and are then almost always ejected from the Solar System. More discoveries may await!

Small as the irregular moons are, they are large compared to the tiniest chunks of rock that have captured Dr. Gladman's interest – and they are right here on Earth. Most of us are familiar with meteorites that have been blasted off the Moon and Mars and then found their way here. But, what about Mercury as a source? Dr. Gladman has determined that impact speeds on that planet are greater than had been assumed and that ejecta leave Mercury at a correspondingly higher velocity. (Mercury is the only planet where impact speeds are characteristically 5 to 20 times the planet's escape velocity). This gets them away from the Sun, propelling some toward Earth. Dr. Gladman believes there may be Mercurian meteorites sitting in collections right now! Some experts have speculated that meteorites known as angrites may be from the inner planet, but Dr. Gladman points out that to be sure, some sort of ground truth from Mercury will be required. The *MESSENGER* probe may provide such information.

The main source of meteorites, however, is the asteroid belt. Early studies suggested that such bodies could be delivered to the terrestrial planets simply through collisional and subsequent gravitational forces. However, Dr. Gladman demonstrated through dynamical studies that their wanderings were of shorter duration than once expected. This caused a complete rethinking of the whole process (in fact, his work has been called a "major blow" against the old theories). Our understanding of the delivery process is now on much firmer ground.

Currently, Dr. Gladman is a member of the Department of Physics and Astronomy at the University of British Columbia and holds the Canada Research Chair in Planetary Astronomy. Among his many awards is the H.C. Urey Prize of the American Astronomical Society's Division of Planetary Sciences. Asteroid 7638 Gladman is named in his honour.

As I write, Jupiter is blazing high in the south. Naturally, it attracts attention even without optical aid, and its study helps inform us about the nature of the Solar System. Clearly, as Dr. Gladman has demonstrated, the smallest objects that orbit the Sun may be put to similar purposes. ✶

Phil Mozel is a past librarian of the Society and was the Producer/Educator at the former McLaughlin Planetarium. He is currently an educator at the Ontario Science Centre.

Imager's Corner

Sub-frame Arithmetic

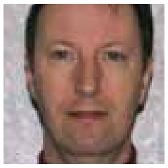

by Blair MacDonald, Halifax Centre
(b.macdonald@ns.sympatico.ca)

This edition's question was sent in by a member from PEI as one of several readers curious about how many exposures to stack.

> *" How many frames do I expose, given that I have somehow managed to figure out how to get a proper exposure? I have assumed from some study 'the more the better'; however, realizing that this is much along the lines of improving SNR by oversampling, there must be some 'point of diminishing returns' after which you're basically wasting time."*

Well the simple answer is – as our questioner surmised – the more images stacked the better. Of course there is a limit to such endeavours and we will have to take a look at what is really going on to see just where the limit is.

First, let's assume, as stated in the question, that each individual frame in the stack is exposed properly. By this I mean that the shutter has been left open long enough so that the sky's photon noise is the dominant noise source in the image. This means that the camera noise can now be ignored. Under these conditions, the data, as sampled at each pixel, can be thought of as the sum of the actual signal plus a zero mean noise signal, or *data* = *signal* + *noise*. Zero-mean random noise is simply a noise that has an average value of zero.

Now there is a branch of statistics that deals with how long it takes a random sequence to settle to its mean value. It turns out that a random process settles to within 10 percent of its mean in about 30 to 35 samples, and to within a percent or two within 80 samples. This is shown in the plot at right (Figure 1a), which is the average of a number of samples generated by a pseudorandom number generator with a mean of zero and a standard deviation of one.

As you can see, the curve flattens out at about sample 15 and is within 10 percent of the mean shortly after that. There is some variability on this (it is random data), and the next run looks different, as shown in Figure 1b. In spite of this random difference, the curve has again flattened out by sample number 30 and is a reasonable approximation of the mean slightly before that.

These plots show that, if you take 20 to 30 exposures that are photon-noise limited, then you have a reasonable average value for each pixel. The short answer, then, is to take as many exposures as you can, but after about 30, you will see very little improvement in the SNR for a rather large increase in the number of exposures. Generally, I shoot between 10 and 30 exposures – 10 for very bright objects where I want detail in the bright areas, and 30 or more for dim Hα nebulae. These numbers are from a dark-sky site; if you shoot in the city or with the Moon up, then you should accumulate additional exposures to reduce the photon noise to acceptable levels. My camera is an unmodified DSLR and is rather insensitive to Hα emissions. Those with a CCD or a modified DSLR may get away with fewer exposures on Hα targets.

Remember, this column will be based on your questions, so keep them coming. You can send them to the list at hfxrasc@lists.rasc.ca, or you can send them directly to me at b.macdonald@ns.sympatico.ca. Please put "IC" as the first two letters in the topic so that my email filters will sort the questions. ✶

Blair MacDonald is an electrical technologist running a research group at an Atlantic Canadian company specializing in digital signal processing and electrical design. He's been an RASC member for 20 years, and has been interested in astrophotography and image processing for about 15 years.

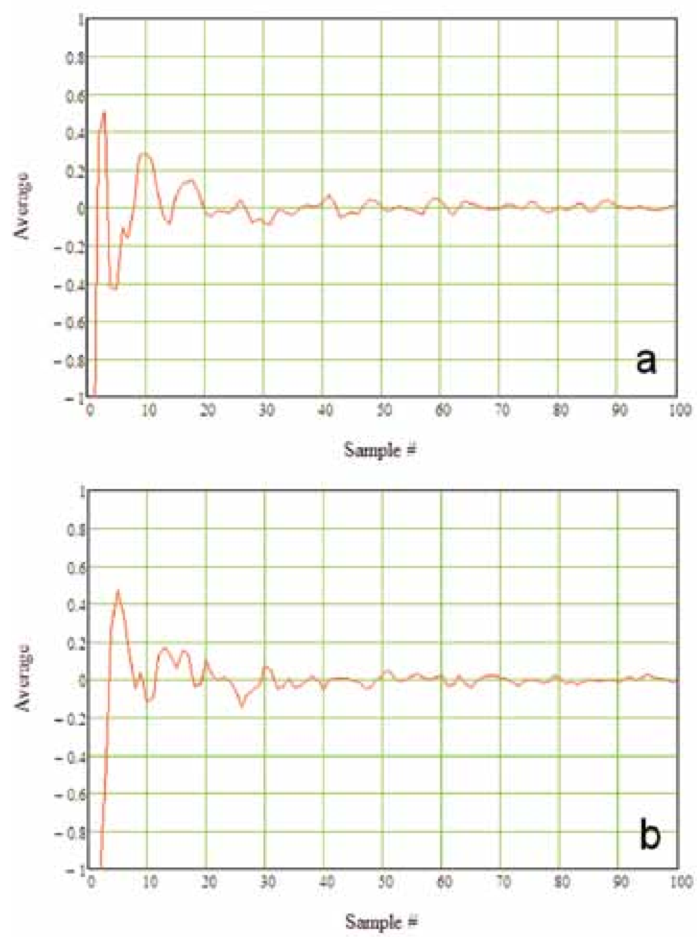

Figure 1 — Random-number sequences showing the gradual convergence to the mean after approximately 30 samples.

Astronomical Art & Artifact

RASC Catalogue of Meteorites — Second Supplement

by R.A. Rosenfeld, RASC Archivist
(randall.rosenfeld@utoronto.ca)

Abstract: A further generous donation has increased the size of the collection and varied its contents, most notably adding fragments of the Tagish Lake (RASC M13) and Whitecourt meteorites (RASC M14), and an NWA lunar achondrite (RASC M16).

Introduction

The RASC Archives have benefitted yet again from the generosity of the anonymous RASC member whose two earlier gifts of meteoritic materials now comprise the majority of the objects in RASC Archive's meteoritical collection (previous material catalogued in Rosenfeld 2009; Rosenfeld 2010). Among the newly added materials are fragments from the Tagish Lake find (RASC M13) and the Whitecourt fall (RASC M14). The collection now also includes a fragment of a lunar meteorite (RASC M16). The space rocks of Canadian provenance and the lunar meteorite are firsts for the collection. The most visually attractive accession is the polished slice of the Admire pallasite (RASC M17). Also joining them is a fragment of possibly the most studied of all the carbonaceous chondrites, Murchison (RASC M15), well-known for the presence of over 100 amino acids, and still the subject of much meteoritical and astrobiological research.

Also included in the gift are several provisionally named meteorites. Should they be evaluated and approved by the Nomenclature Committee of the International Society for Meteoritics and Planetary Science, they will be formally published in the RASC Catalogue.

Catalogue

The catalogue fields consist of:

1. inventory number;
2. type and origin;
3. provenance;
4. dimensions;
5. weight;
6. form;
7. appearance;
8. state of preservation;
9. bibliography (previous publications of a RASC specimen precede general type citations).

Given the limited size of the collection, a little more detail can be supplied in the fields than is usually the case in catalogues. This is not to be taken as a sign of the relative importance of the specimens in the RASC collection; rather it attests to the opposite. It should also be noted that characterizations of the objects are referred to descriptions of the type specimens, or other properly analyzed specimens in the literature, for none of the RASC specimens have been subject to extensive laboratory analysis. This catalogue has been prepared with the needs of the amateur uppermost, rather than the professional.

Meteorites:

19.

1. RASC M13.20110131;
2. Tagish Lake, Carbonaceous chondrite (C2, ungrouped), British Columbia, Canada (59° 42′16″N, 134° 12′5″W), fall 2000 January 18, 10 kg;
3. Anonymous gift 2011 January 31;
4. 16+ fragments; range of fragment sizes ϕ scale=1–3 (Wentworth size class=very coarse sand to fine sand), largest fragment 0.2x0.18x0.17 cm;
5. 0.005 gr;
6. Irregular forms;
7. Colour range: 5PB 2.5/1 Bluish Black Gley to N 2.5/ Black Gley, with sparse inclusions at 5Y 8/1 White (Munsell);
8. Good, but friable as per this type;
9. Not previously published; Hildebrand & McCausland *et al.* (2006); IMCA *EoM* http://www.encyclopedia-of-meteorites.com/meteorite.aspx?id=23782; *MB* 84 (2000), A217-A218; *MBDB* www.lpi.usra.edu/meteor/metbull php?code=23782

20.

1. RASC M14.20110131;
2. Whitecourt, Iron, medium octahedrite (IIIAB), Whitecourt, Alberta, Canada (53° 59′57″N, 115° 35′51″W), find 2007 July 1, ca. 70 kg;
3. Anonymous gift 2011 January 31;
4. 2 fragments: a) 0.448x0.25x0.15 cm; b) 0.23x0.14x0.08 cm;
5. 0.03 gr;
6. 14 a irregular lanceolate form; 14 b irregular form;
7. 14 a & 14 b each have one polished face (treatment happened prior to their separating from a larger mass); weathering rind on other faces;
8. Stable;
9: not previously published; Kofman, Herd & Froese (2010); IMCA *EoM* www.encyclopedia-of-meteorites.com/meteorite.aspx?id=47345; MB94 (2008), 1567; *MBDB* www.lpi.usra.edu/meteor/metbull.php?code=47345 (note: the assigning of an official name to this meteorite post-dates the writing of Whyte 2009).

21.

1. RASC M15.20110131;
2. Murchison, Carbonaceous chondrite (CM2), Murchison, Victoria, Australia (36° 37′S, 145° 12′E), fall 1969 September 28, 4.5 kg;

3. Anonymous gift 2011 January 31;
4. 0.36x0.24x0.2 cm;
5. 0.021 gr.;
6. irregular form;
7. Colour range: 2.5Y 2.5/1 Black to 5Y 2.5/1 Black, with sparse inclusions at 5Y 8/6 Yellow (Munsell);
8. Good;
9. Not previously published; Grady (2000), 351-352; IMCA *EoM* www.encyclopedia-of-meteorites.com/meteorite.aspx?id=16875 ; *MB* 48 (1970), 107-108; *MBDB* www.lpi.usra.edu/meteor/metbull.php?code=16875

22.
1. RASC M16.20110131;
2. Northwest Africa 4734 (NWA 4734), Achondrite (lunar), "Northwest Africa," find October 2006, 1.372 kg;
3. Anonymous gift 2011 January 31;
4. 0.30x0.25x0.175 cm;
5. 0.01 gr.;
6. Irregular form;
7. Note: not a monzogabbro;
8. Good;
9. Not previously published; Wang & Hsu (2010), but see meteorites.wustl.edu/lunar/stones/nwa4734.htm; IMCA *EoM* www.encyclopedia-of-meteorites.com/meteorite.aspx?id=45660; *MB* 93 (2008), 478; *MBDB* www.lpi.usra.edu/meteor/metbull.php?code =45660. Possibly paired with LPA 02205 and 02224

23.
1. RASC M17.20110131;
2. Admire, Pallasite (PMG), Admire, Lyons Co., Kansas, USA (38° 42′N, 96° 6′W), find 1881, 180(?) kg;
3. Anonymous gift 2011 January 31;
4. 2.10x1.49x0.20 cm;
5. 1.176 gr.;
6. Slice;
7. Wide faces polished; typical attractive yellow crystalline olivine inclusions in an iron-nickel matrix;
8. Fragile;

Figure 1 — RASC M17.

9. Not previously published; Grady (2000), 58; IMCA *EoM* www.encyclopedia-of-meteorites.com/meteorite.aspx?id=380; MB 37 (1966), 2; MBDB www.lpi.usra.edu/meteor/metbull.php?code=380

24.
1. RASC M18.20110131;
2. Vaca Muerta, Mesosiderite-A1, Taltal, Antofagasta, Atacama Desert, Chile (25° 45′S, 70° 30′W), find 1861, 3828 kg;
3. Anonymous gift 2011 January 31;
4. 10 fragments; longest fragment 0.57x0.46x0.10 cm; widest fragment 0.549x0.50x0.16 cm; thickest fragment 0.35x0.385x0.20 cm;
5. 0.23 gr.
6. Irregular forms;
7. Weathering crusts;
8. Stable;
9. Not previously published; Grady (2000), 508; IMCA *EoM* www.encyclopedia-of-meteorites.com/meteorite.aspx?id=24142; *MBDB* www.lpi.usra.edu/meteor/metbull.php?code=24142

25.
1. RASC M19.20110131;
2. Tatahouine, Diogenite, Tatahouine, Tunisia (32° 57′N, 10° 25′E), fall 1931 June 27, 12 kg;
3. Anonymous gift 2011 January 31;
4. 3 fragments: a) 0.54x0.35x0.30 cm; b) 0.45x0.38x0.34 cm; c) 0.45x0.15x0.14 cm;
5. 0.131 gr.;
6. Irregular forms;
8. Stable;
9. Not previously published; Grady (2000), 484; IMCA *EoM* www.encyclopedia-of-meteorites.com/meteorite.aspx?id=23884; *MBDB* www.lpi.usra.edu/meteor/metbull.php?code=23884

26.
1. RASC M20.20110131;
2. Gao-Guenie, H5 Ordinary Chondrite, Gao and Guenie, Burkina Faso (11° 39′N, 2° 11′W), fall 1960 March 5 (note: the "second" fall date of April 1960 may be spurious), ? kg;
3. Anonymous gift 2011 January 31;
4. 1.8x1.1x0.35 cm;
5. 1.41 gr;
6. Slice;
8. Fair;
9. Not previously published; Grady (2000), 211; IMCA *EoM* www.encyclopedia-of-meteorites.com/meteorite.aspx?id=10854; *MB* 39 (1970), 91; *MB* 57 (1980), 98; *MB* 83 (1999), A171; *MBDB* www.lpi.usra.edu/ meteor/metbull.php?code =10854

27.
1. RASC M21.20110131;
2. Northwest Africa 6080 (NWA 6080), LL4 Ordinary Chondrite, "Northwest Africa," find 2008, 6.33 kg;
3. Anonymous gift 2011 January 31;
4. 2 fragments: a) 1.025x1.0x0.5 cm; b) 0.3x0.19x0.16 cm;
5. a) 0.667 gr; b) 0.19 gr;
6. Irregular forms;
7. a) has one polished face;
8. Good;
9. Not previously published; IMCA *EoM* www.encyclopedia-of-meteorites.com/meteorite.aspx?id=51489; *MB* 99 (2011) – in preparation; *MBDB* www.lpi.usra.edu/meteor/metbull.php?code=51489

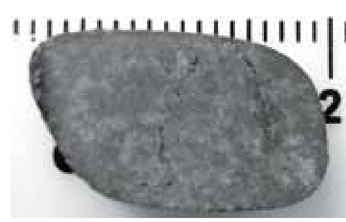

Figure 2 — RASC M20.

28.
1. RASC M22.20110131;
2. Northwest Africa 869 (NWA 869), L 4-6 Ordinary Chondrite, "Northwest Africa," find 2000 (or 2001), 2000 kg;
3. Anonymous gift 2011 January 31;
4. 1.1x0.93x0.77 cm;
5. 1.41 gr;
6. Irregular prolate "spherule";
7. Pebble, with intact fusion crust and discernible regmaglypts;
8. Good;
9. Not previously published; IMCA *EoM* www.encyclopedia-of-meteorites.com/meteorite.aspx?id=31890; *MB* 90 (2006), 1386-1387; *MBDB* www.lpi.usra.edu/meteor/metbull.php?code=31890

Figure 3 — RASC M21.

Addenda and corrigenda to the original catalogue (Rosenfeld 2009):

A document recently come to light has clarified some of the puzzling issues regarding RASC M1 and RASC MWr2. The document is a receipt on Royal Ontario Museum Mineralogy Department letterhead, dated 1974 December 18, addressed to Robin P. Macfarlane of the RASC, and signed by the then curator of mineralogy, J.A. Mandarino, acknowledging the deposit of the specimen B-151 (=RASC M1). It is not known if the meteorite was deposited at the RASC's request for confirmation of the specimen's identity, or the ROM's, as part of a professional study, or both. It will be recalled that RASC M1 is painted with the inventory number "B-151" (=Bruderheim specimen 151), the same number mentioned in the ROM receipt. That document also bears in hand-written annotations substantially the same text as the worn paper label now associated with RASC MWr2: "Bought from U. of Alberta for/$28. in 1961. Identified Dec. 18th/ 1974 by J.A. Mandarino, Curator/Dept. of Mineralogy R.O.M." (Rosenfeld 2009, 211). These facts unequivocally demonstrate that both the newly discovered ROM receipt as well as the worn paper label now associated with RASC MWr2 clearly refer to RASC M1.

Two conclusions can be drawn from this: 1) Mandarino's professional judgement concerning "B-151" was thoroughly sound; and 2), after the close of 1974, someone in the RASC National Office moved the worn paper label from RASC M1 where it belonged to RASC MWr 2, where it clearly didn't. This was done either in complete ignorance, or with mischievous intent.

Acknowledgements:

The author wishes to thank the donor of the anonymous gift of meteorites for reading over this catalogue, the Specula astronomica minima for the generous loan of lab equipment, and the *Journal's* Editor for his forbearance. This research has made use of NASA's Astrophysics Data System. ✶

Abbreviations:

IMCA *EoM*=International Meteorite Collectors Association. Encyclopedia of Meteorites

LPA=La Paz Icefield

M&PS=Meteoritics & Planetary Science

MB=Meteoritical Bulletin

MBDB=Meteoritical Bulletin Database

NWA=Northwest Africa

Manuscripts:

RASC Archives, receipt for deposit of meteorite specimen B-151 [RASC M1] at the ROM Department of Mineralogy, signed by J.A. Mandarino to Robin P. Macfarlane 1974 December 18

References:

Grady, M.M. (2000). *Catalogue of Meteorites: with Special Reference to Those Represented in the Collection of the Natural History Museum, London.* Cambridge-New York: Cambridge University Press

Hildebrand, A.R. & McCausland, P.J.A. *et al.* (2006). The Fall and Recovery of the Tagish Lake Meteorite. *M&PS*, 41, 3, 407-431

Kofman, R.S., Herd, C.D.K., & Froese D.G. (2010). The Whitecourt Meteorite Impact Crater, Alberta, Canada. *M&PS 45*, *9*, 1429-1445

Rosenfeld, R.A. (2009). RASC Catalogue of Meteorites. *JRASC 10*, 5, 208-211

Rosenfeld, R.A. (2010). RASC Catalogue of Meteorites – First Supplement. *JRASC 104*, 2, 80-82

Wang, Y. & Hsu, W. (2010). SIMS PB/PB Dating of ZR-Rich Minerals from NWA 734 and LAP 02205/02224: Evidence for the Same Crater on the Moon. *M&PS 45*, S1, A210

Whyte, A.J. (2009). *The Meteorites of Alberta.* Edmonton: University of Alberta Press

Web sites:

IMCA EoM=International Meteorite Collectors Association. *Encyclopedia of Meteorites.*

www.encyclopedia-of-meteorites.com/ (accessed 2011 February 1)

MBDB=Meteoritical Society. *Meteorite Bulletin Database.*

www.lpi.usra.edu/meteor/metbull.php (accessed 2011 February 1)

The Royal Astronomical Society of Canada is dedicated to the advancement of astronomy and its related sciences; the Journal *espouses the scientific method, and supports dissemination of information, discoveries, and theories based on that well-tested method.*

Second Light

The Most Distant Known Object in the Universe

by Leslie J. Sage
(l.sage@us.nature.com)

As far as we can tell, the Universe began about 13.7 billion years ago with the Big Bang. By the end of the first few minutes, matter had been created, inflation had happened, and the overall properties of the Universe established. Several hundred thousand years later, the Universe had expanded and cooled sufficiently for electrons to combine with protons to form hydrogen atoms. At that time, radiation could stream freely outward, and it is from this time that cosmic microwave background comes. Some hundreds of millions of years later – no one knows for sure how many – the first stars and galaxies began to form. Rychard Bouwens and Garth Illingworth of the University of California-Santa Cruz and their collaborators have now found the most distant known galaxy, at a redshift of z~10 (500 million years after the Big Bang), using data taken by the *Hubble Space Telescope* over the last two summers, after its latest refurbishment (see the January 27 issue of *Nature*).

The previous record holder for the most distant object was the host galaxy of a gamma-ray burst at z~8.2 (which was actually spectroscopically confirmed), and, previous to that, a galaxy at z~7. (There is an unconfirmed, and controversial, claim of spectroscopic identification at z~8.6.) The *Hubble* Ultra Deep Field has revealed many z~7 and z~8 galaxies, and even some at z>8. The chances of clear spectroscopic confirmation of the redshift of galaxies at z>8 are small, at least until the *James Webb Space Telescope* is launched later this decade, or we have a 30-m-class ground-based telescope, or a lucky break with a galaxy with the right properties (such as one that is gravitationally lensed). For now, we are pretty much stuck with *photometric* redshifts.

Photometric redshifts use the fact that some star-forming galaxies are bright in the ultraviolet to identify them. Emission from the Lyman-α line (where an electron is in the first excited state and emits a photon to go to the ground state) or from higher-excited states comes from hot gas, which usually surrounds massive young stars. This emission (and virtually all the shorter wavelength ultraviolet light) is absorbed by intervening hydrogen gas at lower redshifts along the line of sight, causing the galaxy to disappear from view at shorter wavelengths. For a galaxy at a redshift of ~10, the 0.12-microns Ly-α line is redshifted to a wavelength of ~1.3 microns, or well into the near-infrared. That means astronomers have to go a wavelength longer than 1.2 microns for the galaxy to be visible, and only with the most recent upgrade could the *HST* do this at the sensitivity required. In principle, the procedure is quite straightforward: look at the images taken in different wavebands, and when the galaxies start appearing as you move into the infrared, you can approximately tell what the redshift of the galaxy is, under the assumption that the light is mainly from the Ly-α line. In practice, though, the procedure is anything but straightforward. At that distance, galaxies are tiny blobs only a few pixels across, and not much brighter than the background noise. Bouwens and Illingworth therefore set some very conservative criteria on what they would call detection. (A competing group, with less conservative criteria, claims more detections.)

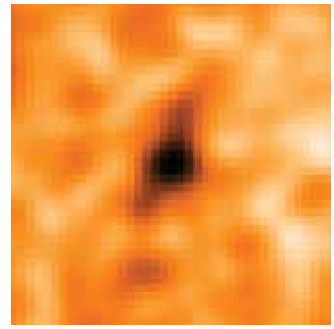

Figure 1 — The H-band images of the one HUDF z~10 candidate. Not much to look at, is it? Image courtesy of Rychard Bouwens, Garth Illingworth, and Nature.

After all of their analysis, Bouwens and his collaborators found one z~10 candidate more than 5σ above the noise, which should be robust. But, it is detected only in one waveband, due to limitations of the telescope detectors, so it is being labelled a *candidate* for now.

One problem that has bedevilled claims in the past is that there is a very strong oxygen line that also arises in star-forming regions, and therefore could fool observers, as it would mean the galaxy lies at only ~$^{1}/_{3}$ of the distance if the line was assumed to be Ly-α. Bouwens believes the galaxies they found are not fooling them, for the following reason: the careful analysis of images taken in many filters (colours) enabled the team to distinguish objects affected by the oxygen line, or dusty galaxies at lower redshift, from the real high-redshift objects. These objects are so faint, though, that minor problems with the detector or noise spikes can also result in spurious objects. *Gotchas* lurk everywhere in this game!

In the *hierarchical accretion* picture that has developed over the past 20 or so years, galaxies start small, and grow through a series of mergers with other small ones. (The past couple of years have seen extensive theoretical discussion also about growth through accretion directly from streams of gas outside the developing galaxies, but for now, we will stick with the widely accepted hierarchical picture as the key to building up galaxies.) Bouwens looked at the average luminosity of galaxies at lower redshifts and asked how many he would likely find if the average brightness at z~10 was the same – the answer is a lot more than what they have seen, and the team concludes that galaxies are evolving very rapidly at that time, which is just 500 million years after the Big Bang. While such evolution is generally expected, the changes are striking – in just 200 million years from z~10 to z~8, the star-formation rate density in the Universe increases tenfold. This suggests that even greater changes will be afoot at redshifts between 10 and 15.

Where do we go from here? There are two important constraints. First is that, as we press to higher redshifts, the galaxies are getting smaller and less luminous. At some point, we will be in the regime of the first stars and the galaxies may be too small and faint to see directly. Secondly, we need telescopes that go further into the infrared, as the *JWST* will do. The best guess right now is that the first stars started forming at z~15-20 or so, about 200 million years earlier, and just 2-300 million years after the Big Bang. Claims of excess infrared emission that would arise from Ly-α emission at such a redshift have been controversial. (To a scientist, *controversial* means that the claim is regarded in a range from skeptical to nonsense.)

The next step is to study the era of *reionization*, where ultraviolet photons from the first stars and galaxies ionized the neutral hydrogen that permeated the Universe after the epoch of recombination, where the electrons and protons combined. The first steps in that direction are now being taken, but that is a story for another day. ✶

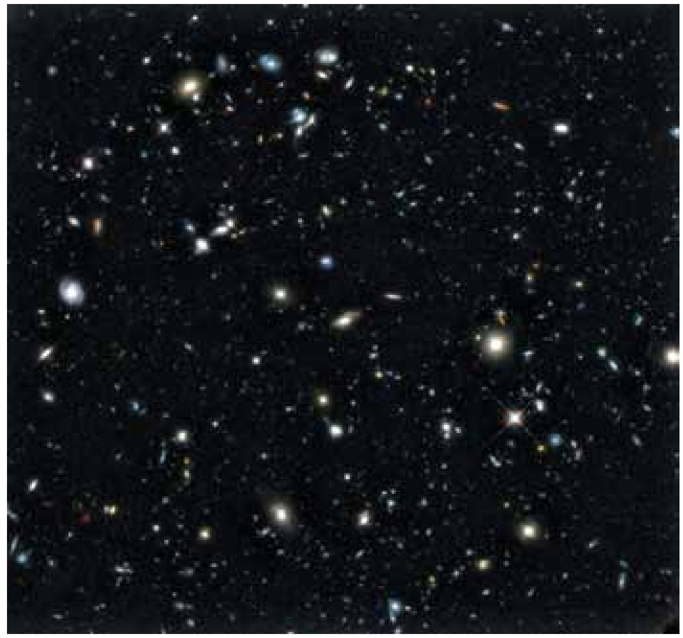

Figure 2 — The Hubble UDF in the near infrared, where three bands have been combined to give colour. It goes down to 29.9 AB mag – that's the magnitude of a 5σ detection in the combined images. (The H-band image alone is "of course" somewhat less sensitive.) Image courtesy of Rychard Bouwens, Garth Illingworth, and Dan Magee.

Leslie J. Sage is Senior Editor, Physical Sciences, for Nature Magazine *and a Research Associate in the Astronomy Department at the University of Maryland. He grew up in Burlington, Ontario, where even the bright lights of Toronto did not dim his enthusiasm for astronomy. Currently he studies molecular gas and star formation in galaxies, particularly interacting ones, but is not above looking at a humble planetary object.*

Brian Segal 1948-2011

To many readers of the *Journal*, Brian Segal was a faceless entity working in the background, doing his "design" thing. But, it is to him that we owe the truly great appearance of our beloved *Journal*; he maintained the style and brand, with his keen knowledge of graphics, eye appeal, balance, and space. It was his choice of fonts, layout, and design that made the *Journal* special. Brian passed away in mid-February as his final issue of the *Journal* was being delivered to readers. It was a struggle to complete, but his dedication to the RASC and to its publications kept him working when less inspired mortals might have paused to rest.

We were especially pleased with his revised front-cover design in the December 2010 issue and intend to continue pressing on with the changes he had envisioned, letting the *Journal* evolve to a more contemporary format.

Brian drew a cartoon, titled The Far Side of Relativity, for nearly every issue. The inane Uncle Ernie, with his loony ideas, will be sorely missed! On occasion, Brian would write a column if material was needed to fill a space. Those few columns revealed a man who had a great fondness for the sky and stars.

Brian's image processing for the *Observer's Calendar* helped make it one of the premier offerings in our stable. He had the talent to make an image sparkle – a talent that is obvious as every new month is revealed when the Calendar pages are turned through the year. His work for the RASC also appears in other places, often anonymously. The RASC ad that graces *SkyNews* magazine was for many years designed by Brian Segal.

We have a very large gap to fill, as we grieve with his family in Antigonish, Nova Scotia. Our deepest condolences go out to Brian's wife, Julia, their daughters, Sarah and Emma, and all of Brian's family.

Through My Eyepiece

Big and Small

by Geoff Gaherty, Toronto Centre
(geoff@foxmead.ca)

Last time around, I gave some suggestions on what might be a good telescope for a 21st-century beginner. This has led me to reflect on what telescopes I actually use myself.

In my basement, I have quite a collection of telescopes: 14 at last count (see www.gaherty.ca/telescopes.htm). The ones I find myself using most often are, strangely enough, the biggest and the smallest.

My big guns are both 280-mm aperture: my Celestron CPC 1100 Schmidt-Cassegrain, which resides in my SkyShed POD most of the time, and my Starmaster 11-inch Dobsonian, which unfortunately doesn't fit in my POD. Because the Celestron is ready to go at a moment's notice, it gets used the most, and I'm very satisfied with the depth and detail of its views, and its very user-friendly computer system.

My second most frequently used telescope is my smallest aperture, my 40-mm Coronado Personal Solar Telescope. This gets used just about every clear day, mounted on a Celestron NexStar mount, which is light, easy to use, and gives me accurate tracking. This is a hydrogen-alpha telescope, and provides me with views of the Sun that none of my other telescopes can manage. There always seems to be something happening on the Sun, even during times of little sunspot activity. There are always prominences and filaments visible, and quite often flares can be seen, as well.

Although most of my nighttime observing is done with my big guns, lately I've been having a lot of fun with some of my smaller telescopes. I'm particularly fond of the three scopes that I wrote about here in February last year *(Fun, Go, and Galileo: Three Low-Priced 'Scopes)*. In particular, I've found that I can hand-hold the little 76-mm FunScope reflector while seated in a garden chair. This is absolutely great for exploring the Milky Way or when the temperature is too low to consider spending much time outdoors.

Over the years, I've owned quite a few telescopes in the 100- to 150-mm aperture range. I like the portability of these scopes, though I often find the views in the smaller ones frustrating. After much agonizing, I've come to the conclusion that 125- to 150-mm apertures can be quite satisfying, but anything smaller just doesn't cut it. I think this is mostly true for *experienced* observers – those whose eyes are already trained to detect detail at the edge of perception. So I still strongly recommend that beginners consider nothing smaller than a 200-mm aperture, 250-mm being better, because beginners need all the help they can get.

Those who've been following my ramblings for a while will know that I've become much more lenient towards GoTo mounts and other electronic aids. The reality of today's astronomy is that most of us live in cities and must contend with light pollution. Computerized telescopes have almost become a necessity.

I'm a bit puzzled about how bad the light pollution is, particularly in the eastern half of North America. If you look at a satellite image that shows light pollution (Figure 1), there's an almost complete split somewhere around the Mississippi River: bright to the east, dark to the west. It looks like someone drew a line from Winnipeg to the southern tip of Texas! It doesn't have to be that bad. My son, who's doing graduate work in Australia, was commenting the other day about how beautiful the stars are in suburban Melbourne. Melbourne is almost the same size as Toronto, so why the difference? Perhaps it's because the rural environs of Melbourne are not lit up anywhere near as brightly as the surroundings of Toronto. ✶

Geoff Gaherty received the Toronto Centre's Ostrander-Ramsay Award for excellence in writing, specifically for his JRASC *column, Through My Eyepiece. Despite cold in the winter and mosquitoes in the summer, he still manages to pursue a variety of observations, particularly of Jupiter and variable stars. Besides this column, he contributes regularly to the* Starry Night Time*s and writes a weekly article on the Space.com Web site.*

Figure 1 — The lights of North America, as seen from a combination of weather satellites. Similar images are available at www.nrlmry.navy.mil/NEXSAT.html. Image: Naval Research Laboratory.

Winnipeg welcomes you to the 52nd General Assembly of the Royal Astronomical Society of Canada, July 1-4, 2011!

We would like to present to you the top 10 reasons we think you should attend the GA in Winnipeg:

Reason #10:
Winnipeg has been a traditional meeting place for the past 6000 years!

Explore the Forks on Friday afternoon, grab dinner and catch the fireworks after the Wine and Cheese!

We're also celebrating a homecoming for several former Winnipeg Centre members!

Reason #9:
You'll get to try out our new airport

Uh, maybe... originally scheduled to open October 2010, delays means it may not actually be open in time for you folks to use it. But you'll get to see it from the runway! Hey, it's only Reason #9...

Reason #8:
Aurora!

Winnipeg is in a prime location to observe the Northern Lights and the increased activity on the Sun means we might get a light show!

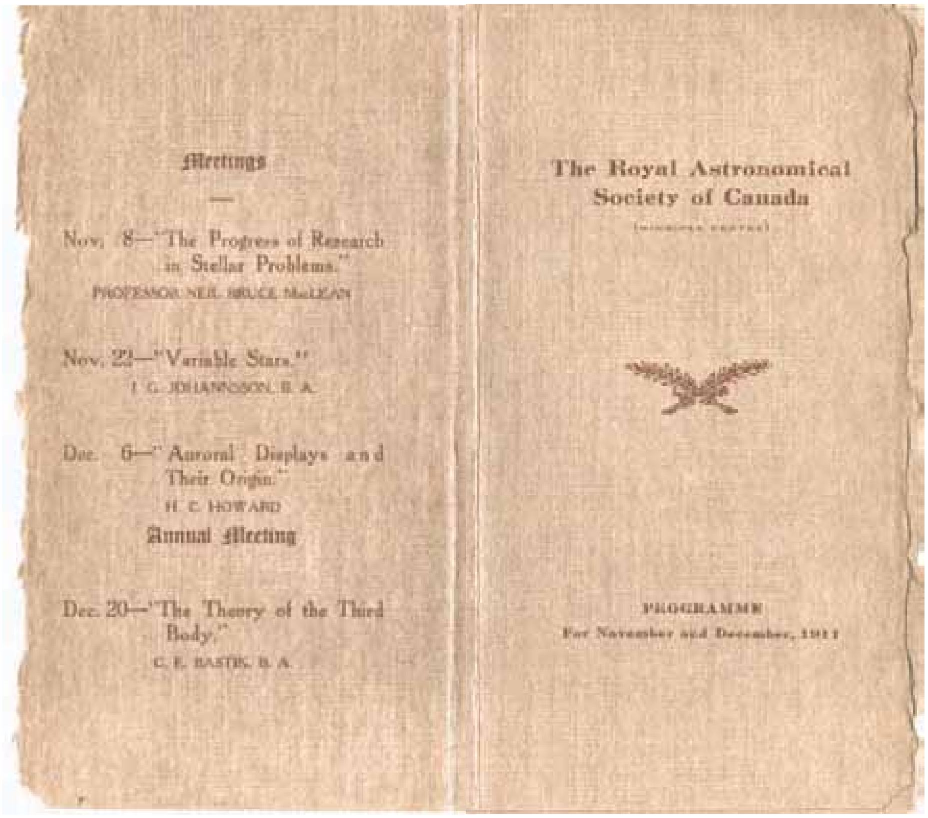

Meetings

Nov. 8—"The Progress of Research in Stellar Problems."
PROFESSOR NEIL BRUCE MacLEAN

Nov. 22—"Variable Stars."
J. G. JOHANNSSON, B. A.

Dec. 6—"Auroral Displays and Their Origin."
H. E. HOWARD

Annual Meeting

Dec. 20—"The Theory of the Third Body."
C. E. BASTIN, B. A.

The Royal Astronomical Society of Canada

(WINNIPEG CENTRE)

PROGRAMME

For November and December, 1911

Reason #6:
New facilities

We are delighted to feature a new residence and new meeting rooms since the University of Manitoba last played host to the GA in 2000.

We have reserved 80 spaces at the Arthur Mauro Residence at the University of Manitoba for $80.90 per night. Older, dormitory-style accommodation is available on a first-come/first-served basis at Mary Speechly Hall for a cost of $46.90 per night. See umanitoba.ca/student/housing/Conference.htm for details and to book your room. Reservations at Arthur Mauro will be held until early May.

Reason #7:
It's a birthday party!

Winnipeg Centre is 100! The first meeting of Winnipeg Centre that we have on record featured a talk entitled "The Progress of Research on Stellar Problems" on November 8, 1911 by Professor Neil Bruce MacLean. Look for a talk with the same name... we're also working on featuring other "then and now" talks.

Reason #5:
Good food

We are excited to offer breakfast and lunch packages through the student-owned Degrees Restaurant in the Student Union building. Great food and reasonable prices! Barbeques and banquets organized as a part of the GA festivities will provide dinner on all days except for Friday, where you can explore the many restaurants and food options at the Forks.

DEGREES

Reason #4:
Amazing arts and culture

Winnipeg is renowned for its arts and culture. Some of you may wish to extend your trip and take in one of North America's premier outdoor music festivals, the Winnipeg Folk Festival, which takes place 2011 July 6-10. A production of the Broadway musical theatre phenomenon, CATS is also being shown at Winnipeg's unique outdoor amphitheatre venue, Rainbow Stage, from June 21 – July 10.

Reason #3:
Our exciting program

We have an amazing program of exciting speakers and great tours to offer you and your family!

Invited Speakers:
Dr. Christine Wilson, McMaster University
Dr. Samar Safi-Harb, Canada Research Chair Tier II University of Manitoba
Alan Dyer, author and astrophotographer
Dr. Paul Delaney, York University

Friday Wine and Cheese at the Manitoba Museum of Man and Nature: The Michelin Green Guide rates the Manitoba Museum as "worth a trip" meaning that the Museum itself is reason enough to come to Winnipeg. We will hold the Wine and Cheese icebreaker in the Museum with access to the galleries by RASC members. The Wine and Cheese is the "fun" part of the GA (or perhaps "silly" part). We'll have contests, music, food, wine and beer, and the July 1st fireworks to help get the General Assembly off to a good start. Expect out-of-this-world prizes for the most enthusiastic competitors.

WINNIPEG FOLK FESTIVAL

RAINBOW STAGE

Tours:

Lower Fort Garry and Lockport: Lower Fort Garry National Historic Site, constructed by the Hudson Bay Company in the early 1800s, is the oldest stone fur-trading post in North America

The Canadian Fossil Discovery Centre: Located in Morden (100 km SW of Winnipeg), this centre houses the largest collection of marine reptile fossils in Canada. Meet "Bruce," a 13-metre mosasaur, the fiercest of all the marine reptiles.

Assiniboine Park and the Winnipeg Zoo: Walk on the wild side by visiting Assiniboine Park Zoo, along the Assiniboine River in Winnipeg. The zoo and the park are among Winnipeg's most popular attractions, with approximately 2645 individual animals of 398 species in its collection.

The Prairie Dog Central Railway: Operating one of the oldest steam locomotives in North America, it is a short-line railway owned and operated by The Vintage Locomotive Society Inc. and it is one of the oldest regularly scheduled vintage operating trains in North America.

Reason #2:
Wide open prairie skies

July is thunderstorm season, and the Prairies are the place to watch them. However, we hope for better weather for our activities, though we might be able to accommodate a few storm chasers. For the statistically inclined, July has an average high of 26° C, a low of 13° C, 71 mm of rain on 11 days, and no snow – ever. Skies are clear about 45% of the days. Mosquitoes are guaranteed if the past weather has had at least normal precipitation, but they aren't too bad in the city.

If we get some clear skies, maybe we'll get in some observing. What better place to observe than where you can see the sky from horizon to horizon!

Reason #1:
Well, next year ***is*** 2012...

Gizmos

Wind in the Desert

by Don Van Akker, Victoria Centre
(dvanakker@gmail.com)

Elizabeth and I are camped near Alamogordo, New Mexico, as I write this in January. We are here for warm sun and clear nights.

It is snowing outside. Big wet flakes have made the desert white. I don't remember this being mentioned in the brochures. It is something we are learning about this place.

The other thing we are learning about is wind. They get serious wind here.

Yet snow and especially wind are not unique to this place. We have wind in Canada, too, and not just in January. I think of a star party in July and the mournful face of a man gazing at his lovely telescope, lying on the ground after the wind blew over his tripod.

That is the image that came to my mind the first time the wind woke us up here as it rocked the trailer. The next morning, I did something about it.

What I had in mind was a *pet stake.* If Rover can't pull it out, maybe the wind can't either. I bought one at Walmart and tried to drive it in beneath the tripod. The packed rock and gravel of the campsite were like concrete.

On to Plan B, a spiral tent stake. This is like a giant corkscrew. You don't drive it in, you turn it in.

It should have worked; it didn't – concrete is concrete.

Plan C was more humble. Nothing tricky, just the biggest rock I could lift. Our campsite had an excellent selection.

The tripod got tied down to the rock (or stake) with a piece of strong cord. The only important thing was that it be tied down tightly without any slack at all. To do that I used a modified trucker's hitch.

The trucker's hitch is used for cinching down loads on trucks, but I expect it is older than the name implies since I have seen it, on old documentary film, used to cinch down the load on a camel. I don't think the guy doing it knew much about trucks. ✶

Don and Elizabeth Van Akker usually observe from their home on Salt Spring Island where it doesn't snow so much. Don would love to hear about what you have done or made to make observing better. Email dvanakker@gmail.com.

Figure 1 — Tie a loop into one end of the cord, wrap once around the rock (or pass it through the eye on the stake) and up over whatever works on the tripod. Bring the other end of the cord through the loop and pull down on it while pulling up on the other side. You now have a two-to-one advantage, as if you were using a pulley. I tightened up on it until the rock was just coming off the ground.

Figure 2 — Squeeze the cord where it comes through the loop to keep it from slipping back.

Figure 3 — Take a bight from the tail end of the cord, pass it around the standing line and back through. Pull up on the loop to draw it tight.

Figure 4 — Tie off the two ends with a half hitch.

Figure 5 — Above is the pet stake, beneath it is the spiral tent stake. Either would work well in firm soil or clay, but if you use the pet stake you'd better have something to pry it out with when you're done!

Astrocryptic Answers

1 V	A	2 R	I	3 A	B	4 L	E	5 S	T	6 A	R	7 S
A	■	A	■	N	■	O	■	I	■	S	■	Y
8 N	A	I	A	D	■	9 W	I	D	G	E	O	N
A	■	L	■	R	■	E	■	E	■	L	■	O
10 L	A	S	S	E	L	L	■	11 S	O	L	I	D
L	■	■	■	W	■	L	■	■	■	U	■	I
12 E	G	13 R	E	S	S	■	14 P	15 A	R	S	E	C
N	■	U	■	■	■	16 H	■	L	■	■	■	P
17 B	O	D	E	18 S	■	19 R	E	M	O	20 R	S	E
E	■	O	■	Y	■	M	■	A	■	A	■	R
21 L	A	L	A	N	D	E	■	22 N	U	N	K	I
T	■	P	■	T	■	R	■	A	■	D	■	O
23 S	C	H	W	A	R	Z	S	C	H	I	L	D

Are you moving? Is your address correct?

If you are planning to move, or your address is incorrect on the label of your *Journal*, please contact the National Office immediately:

(416) 924-7973
www.rasc.ca/contact

By changing your address in advance, you will continue to receive all issues of *SkyNews* and the *Observer's Handbook*.

Society News

by James Edgar, National Secretary
(jamesedgar@sasktel.net)

Some time ago, I was given a large stack of documents (very large!) that had been collected over the years by various National Secretaries: Dr. Randall Brooks, Raymond Auclair, Kim Hay, and Stan Runge – a veritable short history of the recent RASC. They (the documents, not the National Secretaries!) have been lying idly in storage containers, waiting for the day I would finally take a peek; maybe to shred the non-essential items and keep the good stuff. Secretaries are pack rats by nature, so I fully expected to find some Tim Hortons receipts in there! But, no, nothing that esoteric.

One of the "keepers," shown here for your reading pleasure, is a hand-written letter in response to permission from National Office to reproduce the *Observer's Handbook* star maps for a school project. Here it is as I found it, with just the name and address obscured for privacy reasons. I love the pressed flowers captured under clear tape on the letter's margin. Here's hoping the young aspiring astronaut who wrote to Bonnie Bird a few years back somehow gets to read it again!

We have to reach out to those people who write such letters – we must become relevant to them. ✶


RASC
Mrs. Bird
136 Dupont St.
Toronto, ON M5R 1V2

Dear Mrs. Bird,
Hello! You gave me permission a week or so to photocopy a few star maps in the Observers Handbook 2003 for a science project. I just wanted to tell you that several people took the maps home with them, and I believe that this country has a few new (genuinely-interested young) amateur astronomers! :) The project went wonderfully :), and the maps really helped. Thank you again!

Very Sincerely,

Great Images

Orion the Hunter

by Rick Stankiewicz, Unattached Member
(stankiewiczr@nexicom.net)

This night-sky scene has been prominent in the Northern Hemisphere for the past few months, though taken on 2010 October 4 before sunrise in Killbear Provincial Park, near Parry Sound, Ontario. The view shows the familiar constellation of Orion "The Hunter" and his three famous belt stars. Hanging from the belt is the Hunter's sword containing the well-known Orion Nebula (M42), visible here as the middle star of the three "sword" stars. Also visible are the constellation of Taurus the Bull with its iconic V-shaped asterism and, above that, the Pleiades open cluster. To the upper left of Orion is the constellation of Gemini, The Twins. The lighting in this image was from a parking lot, which added to the effect by framing the night sky in the opening between the trees. There are other constellations and parts in this image, too – can you find them? ✶

Photo Details: Tripod-mounted Canon 400D camera and Sigma 10- to 20-mm lens for 1 sec, f/4.0, ISO 1600

THE ROYAL ASTRONOMICAL SOCIETY OF CANADA

NATIONAL OFFICERS AND COUNCIL FOR 2010–2011/CONSEIL ET ADMINISTRATEURS NATIONAUX

Honorary President	Jim Hesser, Ph.D., Victoria
President	Mary Lou Whitehorne, Halifax
1st Vice-President	Glenn Hawley, B.Sc., B.Ed., Calgary
2nd Vice-President	Colin Haig, B.Sc., M.Sc., Hamilton
Secretary/Recorder	James Edgar, Regina
Treasurer	Mayer Tchelebon, MBA, CMA, Toronto
Past Presidents	Dave Lane, Halifax and Scott Young, B.Sc., Winnipeg
Editor of Journal	Jay Anderson, B.Sc., MNRM, Winnipeg
Editor of Observer's Handbook	David M.F. Chapman, M.Sc., Halifax
Editor of The Beginner's Observing Guide	Mary Lou Whitehorne, Halifax
Editor of Observer's Calendar	Dave Lane, Halifax
Executive Director	Deborah Thompson, CAE, Toronto

CENTRE ADDRESSES/ADRESSES DES CENTRES

The most current contact information and Web site addresses for all Centres are available at the Society's Web site: www.rasc.ca

Belleville Centre
c/o Greg Lisk, 11 Robert Dr
Trenton ON K8V 6P2

Calgary Centre
c/o Telus World of Science, PO Box 2100
Stn M Location 73
Calgary AB T2P 2M5

Charlottetown Centre
c/o Brian Gorveatt,
316 N Queen Elizabeth Dr
Charlottetown PE C1A 3B5

Edmonton Centre
c/o Telus World of Science
11211 142 St
Edmonton AB T5M 4A1

Halifax Centre
PO Box 31011, Halifax NS B3K 5T9

Hamilton Centre
c/o Mr. A. Blanchard, 2266 Lakeshore Rd W
Oakville ON L6L 1G8

Kingston Centre
PO Box 1793, Kingston ON K7L 5J6

Kitchener-Waterloo Centre
305 - 20 St George St, Kitchener ON N2G 2S7

London Centre
c/o Peter Jedicke, 82 Barrydale Cres
London ON N6G 2X4

Mississauga Centre
PO Box 98011, 2126 Burnhamthorpe Rd W
Mississauga ON L5L 5V4

Centre francophone de Montréal
C P 206, Station St-Michel
Montréal QC H2A 3L9

Montréal Centre
18455 Meloche St
Pierrefonds QC H9K 1N6

New Brunswick Centre
c/o Paul Gray, 1068 Kingsley Rd
Birdton NB E3A 6G4

Niagara Centre
PO Box 4040
St. Catharines ON L2R 7S3

Okanagan Centre
PO Box 20119 TCM
Kelowna BC V1Y 9H2

Ottawa Centre
1363 Woodroffe Ave, PO Box 33012
Ottawa ON K2C 3Y9

Prince George Centre
7365 Tedford Rd
Prince George BC V2N 6S2

Québec Centre
2000 Boul Montmorency
Québec QC G1J 5E7

Regina Centre
PO Box 20014
Regina SK S4P 4J7

St. John's Centre
c/o Randy Dodge, 206 Frecker Dr
St. John's NL A1E 5H9

Sarnia Centre
c/o Marty Cogswell, 6723 Pheasant Ln
Camlachie ON N0N 1E0

Saskatoon Centre
PO Box 317 RPO University
Saskatoon SK S7N 4J8

Sunshine Coast Centre
5711 Nickerson Road
Sechelt BC V0N3A7

Thunder Bay Centre
286 Trinity Cres
Thunder Bay ON P7C 5V6

Toronto Centre
c/o Ontario Science Centre
770 Don Mills Rd
Toronto ON M3C 1T3

Vancouver Centre
1100 Chestnut St
Vancouver BC V6J 3J9

Victoria Centre
3046 Jackson St
Victoria BC V8T 3Z8

Windsor Centre
c/o Greg Mockler
1508 Greenwood Rd
Kingsville ON N9V 2V7

Winnipeg Centre
PO Box 2694
Winnipeg MB R3C 4B3

Great Images

Lynn Hilborn of the Toronto Centre photographed these giant molecular cloud and dust lanes in Perseus from her WhistleStop Observatory at Grafton, Ontario, in exposures lasting a total of 18 hours for this two-frame mosaic. In the upper right is NGC 1333; above centre and glowing in hydrogen-inspired red is IC 348, an area of star birth surrounded by dark lanes of cosmic dust. Lynn used a Televue NP 101 telescope at f/4.3 and a FLI ML8300 camera equipped with LRGB and Hα filters (binned 1x1).

Journal